

# Catalyst Nuclearity Effects in Olefin Polymerization. Enhanced Activity and Comonomer Enchainment in Ethylene + Olefin Copolymerizations Mediated by Bimetallic Group 4 Phenoxyiminato Catalysts

Michael R. Salata and Tobin J. Marks\*

Department of Chemistry, Northwestern University, Evanston, Illinois 60208-3113

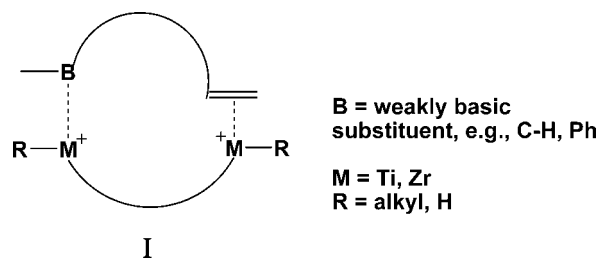
Received September 11, 2008; Revised Manuscript Received December 29, 2008

**ABSTRACT:** This contribution describes the synthesis, characterization, and catalytic implementation of the binuclear {2,7-di-[(2,6-diisopropylphenyl)imino]-1,8-naphthalenediolato} group 4 metal complexes {1,8-(O)<sub>2</sub>C<sub>10</sub>H<sub>4</sub>-2,7-[CH=N(2,6-<sup>i</sup>Pr<sub>2</sub>C<sub>6</sub>H<sub>3</sub>)<sub>2</sub>]}Zr<sub>2</sub>Cl<sub>6</sub>(THF)<sub>2</sub> (**FI<sup>2</sup>-Zr<sub>2</sub>**) and {1,8-(O)<sub>2</sub>C<sub>10</sub>H<sub>4</sub>-2,7-[CH=N(2,6-<sup>i</sup>Pr<sub>2</sub>C<sub>6</sub>H<sub>3</sub>)<sub>2</sub>]}Ti<sub>2</sub>Cl<sub>6</sub>(THF)<sub>2</sub> (**FI<sup>2</sup>-Ti<sub>2</sub>**) in comparison to the mononuclear analogues {3-<sup>i</sup>Bu-2-(O)C<sub>6</sub>H<sub>3</sub>CH=N(2,6-<sup>i</sup>Pr<sub>2</sub>C<sub>6</sub>H<sub>3</sub>)}ZrCl<sub>3</sub>(THF) (**FI-Zr<sub>1</sub>**) and {3-<sup>i</sup>Bu-2-(O)C<sub>6</sub>H<sub>3</sub>CH=N(2,6-<sup>i</sup>Pr<sub>2</sub>C<sub>6</sub>H<sub>3</sub>)}TiCl<sub>3</sub>(THF) (**FI-Ti<sub>1</sub>**), in ethylene homopolymerization and ethylene + olefin copolymerization processes. The comonomers studied include 1-hexene, 1-octene, 1,5-hexadiene (**1,5-HD**), 1,4-pentadiene (**1,4-PD**), and highly hindered 1,1-disubstituted methylenecyclopentane (**MCP**) and methylenecyclohexane (**MCH**). In ethylene + 1-hexene copolymerizations, **FI<sup>2</sup>-Zr<sub>2</sub>** enchains 1.5× more 1-hexene than **FI-Zr<sub>1</sub>**, and **FI<sup>2</sup>-Ti<sub>2</sub>** enchains 2.2× more 1-hexene than **FI-Ti<sub>1</sub>**. While ethylene + **1,5-HD** and ethylene + **1,4-PD** copolymerizations mediated by **FI<sup>2</sup>-Zr<sub>2</sub>** and **FI-Zr<sub>1</sub>** produce ethylene + **1,4-PD** and ethylene + **1,5-HD** copolymers at respectable activities, **FI<sup>2</sup>-Ti<sub>2</sub>** and **FI-Ti<sub>1</sub>** are virtually inactive. While **MCP** and **MCH** are efficiently coenchainment with ethylene via a ring-unopened pathway by both **FI<sup>2</sup>-Ti<sub>2</sub>** and **FI-Ti<sub>1</sub>**, **FI<sup>2</sup>-Zr<sub>2</sub>** and **FI-Zr<sub>1</sub>** produce only polyethylene. These examples represent the first olefin copolymerizations reported for monophenoxyiminato group 4 complexes, and in general the bimetallic catalysts incorporate between 1.8× and 3.4× more comonomer in ethylene + olefin copolymerizations than their monometallic counterparts. In comparison to mono- and binuclear group 4 constrained geometry catalysts (CGCs), the mono- and binuclear **FI** catalysts: (1) enchain significantly greater densities of α-olefins, (2) display enhanced binuclear catalyst polymerization activity versus their mononuclear analogues, and (3) produce predominantly linear polyethylenes as opposed to the branched polyethylenes produced by CGCs.

## Introduction

Recently, intensive efforts have been devoted to discovering unique and/or more efficient metal-centered homogeneous catalytic processes which derive from cooperative effects realizable between proximate active centers in multinuclear metal complexes.<sup>1</sup> In some cases, these complexes mimic the capabilities of enzymes in enforcing conformational control to promote selectivity as well as in enhancing effective local reagent concentrations.<sup>2</sup> In the area of single-site olefin polymerization catalysis,<sup>3</sup> we recently reported that -CH<sub>2</sub>CH<sub>2</sub>- (Chart 1, **Ti<sub>2</sub>**, **Zr<sub>2</sub>**) and -CH<sub>2</sub>- (Chart 1, **C1-Ti<sub>2</sub>**, **C1-Zr<sub>2</sub>**) bridged bimetallic “constrained geometry catalysts” (CGCs)<sup>4</sup> exhibit pronounced nuclearity effects in terms of enhanced branch formation, α-olefin comonomer enchainment selectivity/activity, and molecular weight enhancement as compared to their mononuclear counterparts (Chart 1, **Ti<sub>1</sub>**, **Zr<sub>1</sub>**).<sup>3b,5</sup> Secondary interactions between weakly basic monomer substituents (e.g., C-H bonds, Ph groups) and the second metal center appear to play a key role in modifying enchainment and chain transfer kinetics (**I**). The shorter linker in the **C1**-bridged catalysts draws the catalytic centers to an approximate, shortest attainable M···M distance of ~6.0 Å versus ~6.6 Å in **Ti<sub>2</sub>** and **Zr<sub>2</sub>**.<sup>6</sup> The result of shortening the M···M distance dramatically increases product *M<sub>w</sub>* and 1-hexene enchainment selectivity in copolymerizations.<sup>5c,d</sup>

In the nonmetallocene area of single-site polymerization catalysis,<sup>7</sup> new families of group 4 bis-<sup>8</sup> and monophenoxyiminato<sup>9</sup> olefin polymerization catalysts (Chart 2) have been studied in several laboratories. Attractions of these catalysts include the ease of preparation, activities competitive with those of group 4 metallocenium catalysts, ability to support living polymerizations, and utility in producing unique polyolefin architectures.<sup>10</sup> A priori, the coordinatively open nature of monophenoxyiminato group 4 active sites would appear to be conducive to the enchainment of α-olefin comonomers. However, monophenoxyiminato group 4 catalysts curiously exhibit limited productivity



**B** = weakly basic substituent, e.g., C-H, Ph

**M** = Ti, Zr  
**R** = alkyl, H

and comonomer incorporation selectivity in ethylene + α-olefin copolymerizations.<sup>9</sup> In light of the aforementioned results in which binuclear CGCs exhibit enhanced homopolymerization activities and copolymerization selectivities, the intriguing question arises as to whether two covalently linked phenoxyiminato group 4 catalytic centers could enhance/modify copolymerization productivity and comonomer enchainment selectivity in such polymerizations. In a preliminary communication, we briefly reported the synthesis and initial observations on the polymerization characteristics of the first binuclear phenoxyiminato group 4 metal complex (**FI<sup>2</sup>-Zr<sub>2</sub>**, Chart 3).<sup>11</sup> We synthesized the rigid, planar **FI<sup>2</sup>** ligand to maximize the potential for cooperativity between active phenoxyiminato catalytic centers. The naphthalenic backbone should prevent the metal centers from rotating away from each other during catalytic events as in the flexible alkylene linkers of **Ti<sub>2</sub>**, **Zr<sub>2</sub>**, **C1-Ti<sub>2</sub>**, and **C1-Zr<sub>2</sub>**. In addition to conformational rigidity, the minimum attainable M···M proximity was also taken into account in ligand design. The M···M distance in the **FI<sup>2</sup>** ligand structure is estimated to be 5.4 - 5.9 Å,<sup>12</sup> versus ~6.0 Å for **C1-Zr<sub>2</sub>** and ~6.6 Å for **Zr<sub>2</sub>**.<sup>6</sup> In the aforementioned binuclear CGC systems, shortening the M···M distance via replacing a two carbon linker (**Zr<sub>2</sub>**) with a one carbon linker (**C1-Zr<sub>2</sub>**) leads to dramatic enhancements in polyethylene *M<sub>w</sub>*s and comonomer incorporation densities in the products obtained from **C1-Zr<sub>2</sub>** versus **Zr<sub>2</sub>**.<sup>13</sup>

An additional, informative class of comonomers to examine for cooperative enchainment effects is the highly encumbered methylenecycloalkanes (**MCA**s).<sup>5b,14</sup> For monomers having little or

\* Corresponding author. E-mail: t-marks@northwestern.edu.

Chart 1

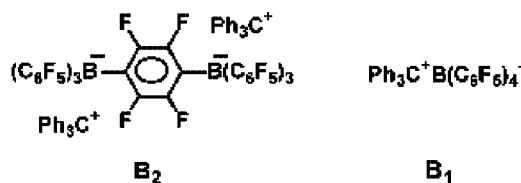
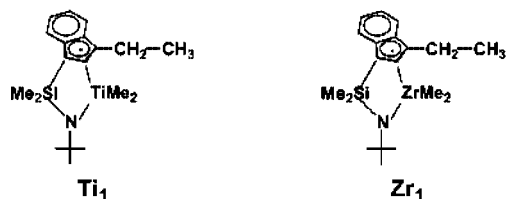
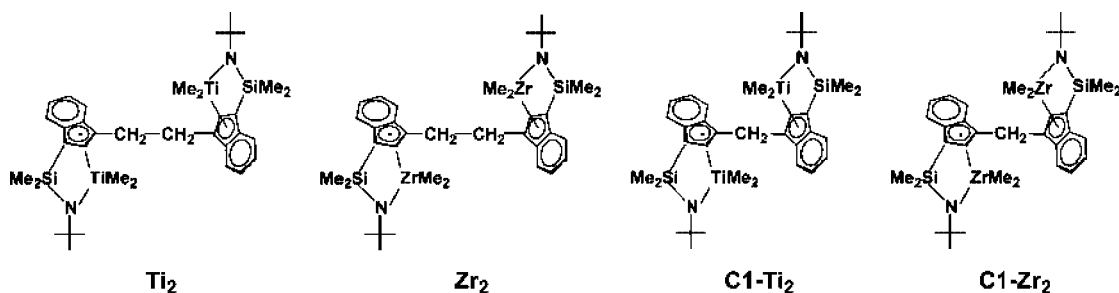


Chart 2

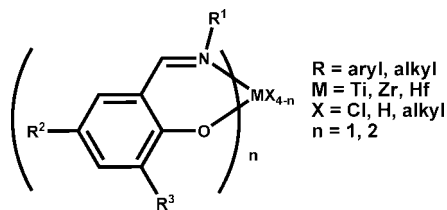
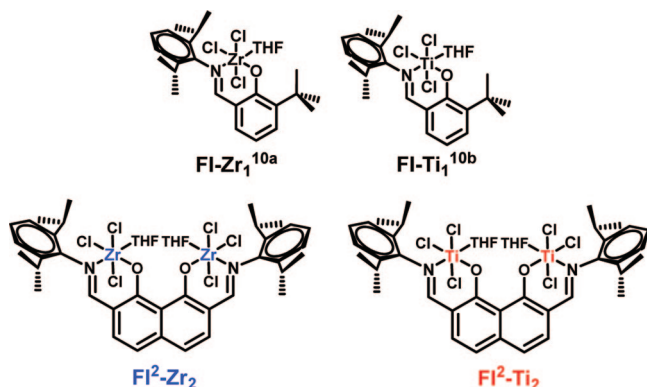


Chart 3

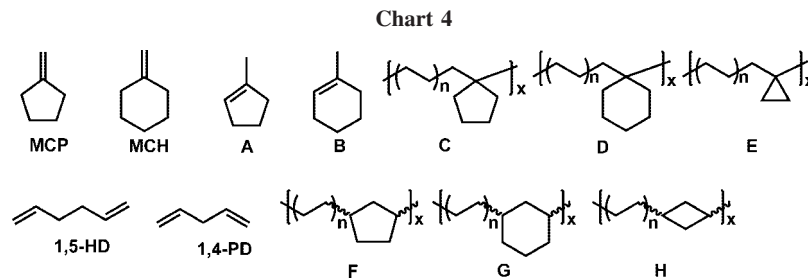


no ring strain such as methylenecyclopentane (MCP) and methylenecyclohexane (MCH), isomerization to the thermodynamically more stable internal cycloolefins (Chart 4, **A,B**) is mediated by a variety of mononuclear  $d^0/f^n$  metallocene catalysts.<sup>14</sup> We recently reported that  $Ti_2$ -mediated copolymerization of MCP and MCH with ethylene leaves the saturated hydrocarbon ring structures intact.<sup>5b</sup> In contrast to highly ring-strained cyclopropyl substituents, comonomers MCP and MCH have minimal ring strain (6.5 and 0 kcal/mol for MCP and MCH, respectively)<sup>14c,15</sup> and can be incorporated into polyethylene chains in ring-unopened geometries. Macromolecules having saturated hydrocarbon rings incorporated in the polyolefin backbone (Chart 4, structures **C,D,E**)<sup>14b,16</sup> are expected to have drastically modified viscoelastic properties, because the bulky rings inhibit the tight coiling effects normally exhibited by polyethylenes. Increasing the average chain length between coils should lessen the tightness of the coiling.<sup>17</sup> Saturated ring-functionalized polyolefins are also expected to have smaller dielectric constants, lower refractive indices, reduced water absorption, and greater optical transparency versus their ho-

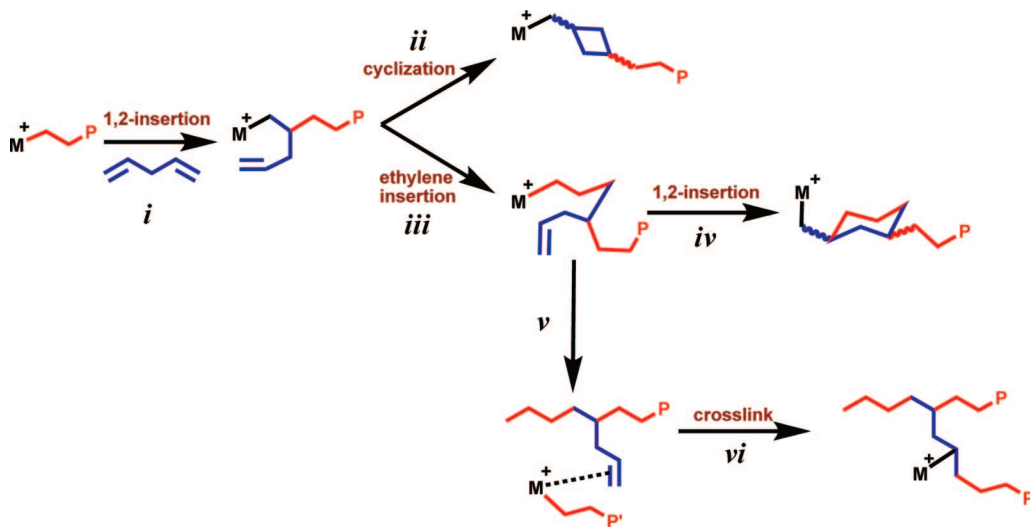
mopolymer counterparts.<sup>18</sup> Since the binuclear catalyst  $FI^2-Zr_2$  exhibits enhanced selectivity for  $\alpha$ -olefin comonomers, the question also arises as to whether this unusual selectivity pattern can be extended to severely encumbered comonomers, and to  $FI^2-Ti_2$ .

Another comonomer class which can introduce saturated hydrocarbon ring structures into polyethylene chains and which may be amenable to cooperative effects is  $\alpha,\omega$ -dienes.<sup>19</sup> In ethylene + 1,5-hexadiene (**1,5-HD**) copolymerizations mediated by zirconocenium catalysts,<sup>20</sup> 1,3-cyclopentyl fragments (Chart 4, structure **F**) are introduced via a diene olefinic group undergoing insertion, followed by rapid cycloinsertion of the second pendant vinyl group. In ethylene + 1,4-pentadiene (**1,4-PD**) copolymerizations mediated by zirconocenium catalysts (Scheme 1),<sup>21</sup> a 1,3-cyclohexyl unit (Chart 4, structure **G**) is introduced via diene olefinic endgroup insertion step (*i*), followed by insertion of an ethylene monomer (step *iii*), then cyclization (step *iv*). Cycloinsertion to afford 1,3-cyclobutyl groups has also been observed (step *ii* and Chart 4, structure **H**).<sup>21a</sup> For **1,5-HD** and **1,4-PD**, the pendant vinyl group may also remain intact as a branch, or may undergo insertion at a second propagating catalyst center to create a cross-link.<sup>21</sup> The highly open, bifunctional nature of  $FI^2-Zr_2$  and  $FI^2-Ti_2$  led us to also investigate ethylene copolymerizations with these two dienes, mediated by the  $FI^2-M_2$  versus  $FI-M_1$  catalysts.

Herein we report the synthesis, characterization, and catalytic polymerization/copolymerization properties of the new binuclear phenoxyiminato precatalysts  $FI^2-Zr_2$  and  $FI^2-Ti_2$ . We compare their polymerization properties to those of the mononuclear analogues  $FI-Zr_1$  and  $FI-Ti_1$  and to the nuclearity effects previously observed in the CGC catalyst series.<sup>5,11,13,22</sup> Studies of ethylene homopolymerization are first discussed, followed by ethylene copolymerizations with the  $\alpha$ -olefins 1-hexene and 1-octene. Next, the hindered olefins MCP and MCH are examined in copolymerizations with ethylene. These results represent the first reports of copolymerizations mediated by monophenoxyiminato Ti and Zr catalysts. It will be seen that, compared to the mononuclear catalysts  $FI-Zr_1$  and  $FI-Ti_1$ , bimetallic catalysts  $FI^2-Zr_2$  and  $FI^2-Ti_2$  produce copolymers with greater efficiency and with significantly greater comonomer enchainment selectivity. Finally, we compare and contrast these results to those obtained with mononuclear and binuclear Ti and Zr CGC catalyst systems.



Scheme 1. Insertion Pathways Established for Ethylene + 1,4-PD Copolymerizations Mediated by Zirconocenium Catalysts<sup>21</sup>



## Results

The goal of this study was to investigate the generality and scope of nuclearity and cooperativity effects in binuclear group 4 olefin polymerization catalysis. For this study, we designed and synthesized a new family of *noncyclopentadienyl* bimetallic group 4 phenoxyiminato complexes to probe the generality of the ‘bimetallic effect’ first identified in CGC-group 4 complexes.<sup>5,13,22</sup> There, covalently tethered CGC centers (Chart 1) exhibit enhanced polymerization activity, selectivity for copolymerization, and product molecular weight. We now sought to assess the consequences of (1) deleting the cyclopentadienyl ligation, (2) contracting the M···M distance, (3) rigidifying the metal binding, and (4) introducing phenoxyimine ligation. The new family of bimetallic complexes synthesized were the phenoxyiminato group 4 complexes, {1,8-(O)<sub>2</sub>C<sub>10</sub>H<sub>4</sub>-2,7-[CH=N(2,6-*i*Pr<sub>2</sub>C<sub>6</sub>H<sub>3</sub>)<sub>2</sub>]}Zr<sub>2</sub>Cl<sub>6</sub>(THF)<sub>2</sub> (Chart 3, **FI<sup>2</sup>-Zr<sub>2</sub>**) and the analogous titanium complex {1,8-(O)<sub>2</sub>C<sub>10</sub>H<sub>4</sub>-2,7-[CH=N(2,6-*i*Pr<sub>2</sub>C<sub>6</sub>H<sub>3</sub>)<sub>2</sub>]}Ti<sub>2</sub>Cl<sub>6</sub>(THF)<sub>2</sub> (Chart 3, **FI<sup>2</sup>-Ti<sub>2</sub>**). It will be seen that increasing the nuclearity of these phenoxyiminato group 4 complexes significantly enhances activity and increases comonomer enchainment selectivity, and that Ti vs Zr polymerization activities and selectivities are quite different.

**I. Synthesis and Characterization of Binucleating Diphenoxymine Ligand Precursor 2,7-Di(2,6-diisopropylphenyl)imino-1,8-dihydroxynaphthalene (**H<sub>2</sub>-FI<sup>2</sup>**).** The precursor to the present ligand, 2,7-diformyl-1,8-dihydroxynaphthalene (**2**), was synthesized according to the literature procedure<sup>23</sup> with minor modifications (see Supporting Information for details). Pure 2,7-diformyl-1,8-bis(methyloxymethoxy)naphthalene (**1**) was obtained by following the procedure outlined by Glaser et al., however after workup, purification of the orange crude product was achieved by repeated washing with ethanol to afford the bright yellow product. The binucleating diphenoxymine ligand, **H<sub>2</sub>-FI<sup>2</sup>**, was synthesized from **2** following the general

condensation methodology outlined by Grubbs et al. for phenoxyimine ligands (eq 1).<sup>24</sup> Under reflux in dichloromethane, condensation of 2,6-diisopropylaniline and **2** in the presence of formic acid as a catalyst and molecular sieves as a water scavenger favors the formation of **H<sub>2</sub>-FI<sup>2</sup>** in good yield. Removal of excess 2,6-diisopropylaniline was accomplished here by repeated washing of the reaction residue with hexanes. The unexpected <sup>1</sup>H NMR spectral characteristics of **H<sub>2</sub>-FI<sup>2</sup>** (see the Experimental Section in the Supporting Information for data) include magnetically inequivalent hydroxyl protons far downfield and a broad, dissymmetric aromatic region. Treatment of **H<sub>2</sub>-FI<sup>2</sup>** with D<sub>2</sub>O results in the immediate disappearance of the two resonances in the <sup>1</sup>H NMR spectrum at δ 13.5 and 14.7 ppm, indicating that they are -OH protons. Recording the spectrum over a temperature range (0 to 140 °C) reveals a dynamic process (Figure 1), and in conjunction with the single crystal X-ray structure, indicates that the structure of **H<sub>2</sub>-FI<sup>2</sup>** is instantaneously dissymmetric and fluxional in solution (see eq 2 and

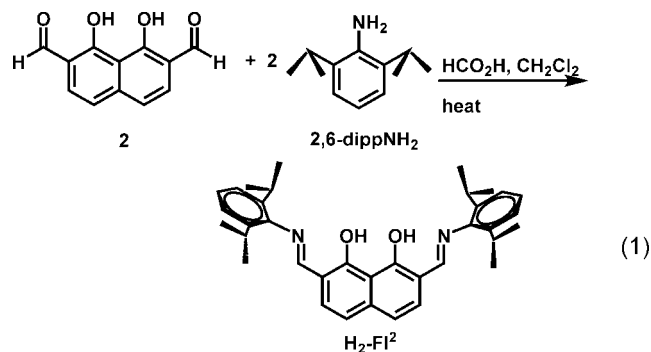
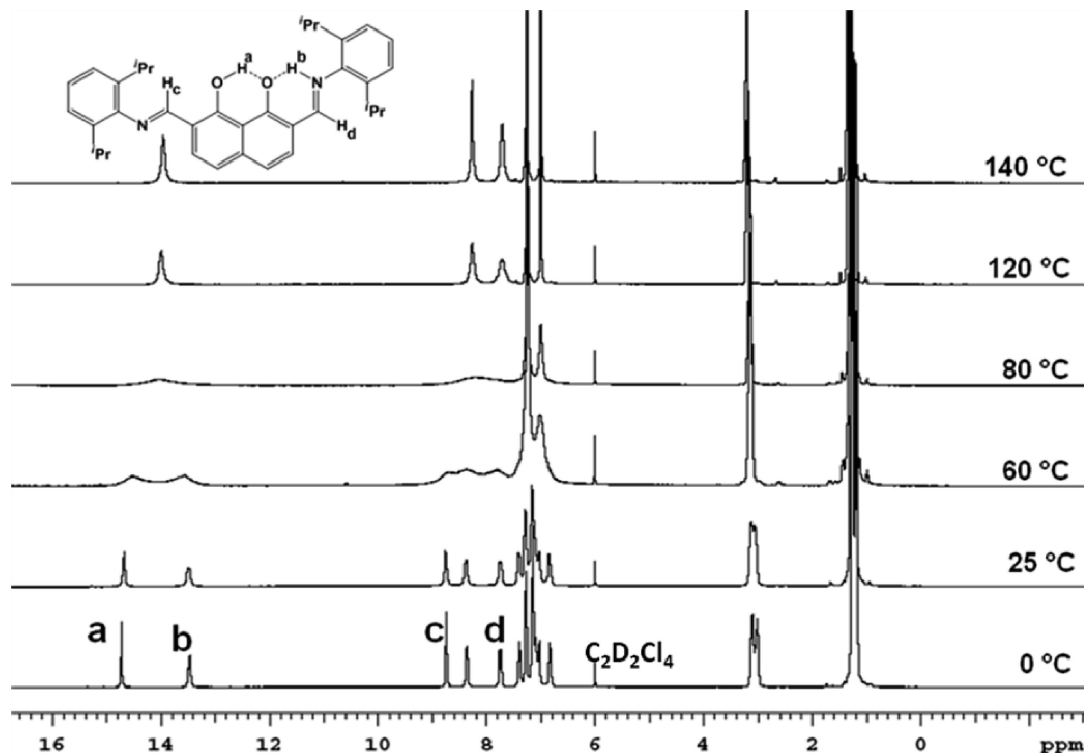
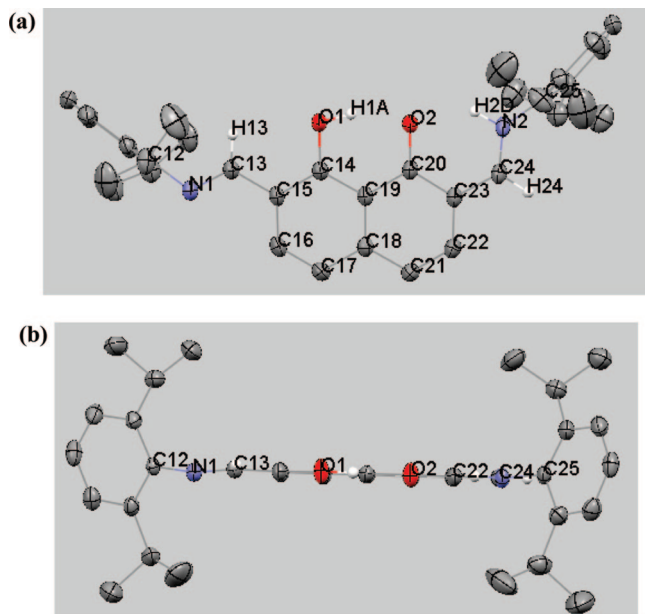


Figure 2, below), with an imine N being reversibly protonated/deprotonated by the adjacent hydroxyl group. At 0 °C, the proton

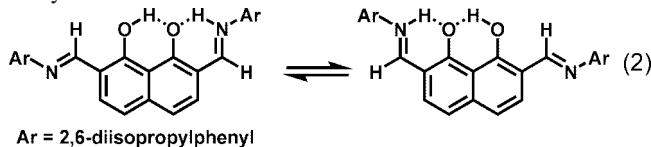


**Figure 1.** Variable-temperature  $^1\text{H}$  NMR (400 MHz) spectra of ligand  $\text{H}_2\text{-FI}^2$  in  $\text{C}_2\text{D}_2\text{Cl}_4$  solution showing dynamic proton exchange between 0 to 140  $^\circ\text{C}$ .



**Figure 2.** Molecular structure and atom numbering scheme for 2,7-di(2,6-di-isopropylphenyl)imino-1,8-dihydroxynaphthalene ( $\text{H}_2\text{-FI}^2$ ). Thermal ellipsoids are drawn at the 50% probability level. (a) Top view of the naphthyl skeleton, and (b) side view of the naphthyl plane. Selected bond distances ( $\text{\AA}$ ) include the following:  $\text{N1}-\text{C13} = 1.279(2)$ ,  $\text{O1}-\text{C14} = 1.3472(19)$ ,  $\text{O2}-\text{C20} = 1.289(2)$ ,  $\text{C24}-\text{N2} = 1.306(2)$ . exchange is slow enough on the NMR time scale that one dissymmetric species is detected, and the peaks are sharp. This low temperature spectrum may be assigned to a solution structure which is the same as the solid state structure, i.e. where one imine N is protonated by the adjacent hydroxyl group, and the other imine N-aryl group is not protonated and is bent away from the hydroxyl group (see eq 2 and Figure 2 below). The doublet at  $\delta$  13.5 ppm is assigned as the hydrogen bound to nitrogen, and it is coupled ( $^3J_{\text{H-H}} = 12.7$  Hz) to the doublet at

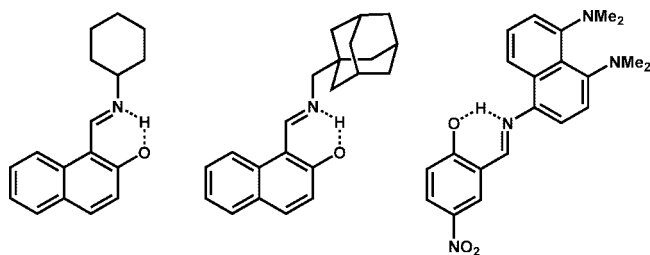
$\delta$  7.8 ppm. The singlets at  $\delta$  12.4 and 8.8 ppm are assigned as the hydroxyl proton and the imine C-H proton which is bent away from the



naphthyl core, respectively. As the solution is warmed in the NMR spectrometer, a number of peaks progressively broaden and by  $\sim 80$   $^\circ\text{C}$  have coalesced. Above  $\sim 80$   $^\circ\text{C}$ , these peaks sharpen as expected for a dynamic process. Above 120  $^\circ\text{C}$ , the two signals for the acidic protons have merged to a single peak, the aromatic region has simplified from eight signals to four, and the signals for the isopropyl groups merge to one peak each for the  $-\text{CH}$  (septet) and  $-\text{CH}_3$  (doublet) groups.

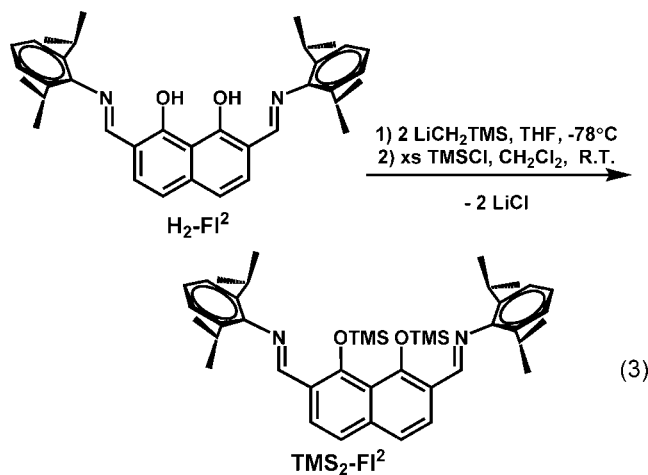
**II. Molecular Structure of Ligand  $\text{H}_2\text{-FI}^2$ .** A summary of crystal structure data for the ligand  $\text{H}_2\text{-FI}^2$  is presented in Table S1 in the Supporting Information, selected bond distances and angles for  $\text{H}_2\text{-FI}^2$  are summarized in Table S2 in the Supporting Information, and a drawing is shown in Figure 2. The imine and hydroxyl hydrogen atoms of the molecule (Figure 2; H1a, H2d, H13, and H24) were located in the difference map, while the remaining hydrogen atoms were placed in idealized positions. As mentioned above, the imine substituents adopt dissymmetric positions relative to the naphthalene core. One imine substituent is protonated, causing it to be drawn proximate to the naphthalene core by a H-bonding interaction with the adjacent deprotonated O atom. This half of the molecule is keto-amine in nature, with the C-O bond being slightly shorter (1.289(2)  $\text{\AA}$ ) and having double bond character relative to other phenoxyimine C-O bonds (1.355(2)  $\text{\AA}$ ). This type of keto-amine structure in the solid state has been described in at least three other examples of phenoxyimine molecules (Scheme 2).<sup>25</sup> The neighboring imine substituent is not protonated, and is consequently bent away from the hydroxyl region due to the absence

Scheme 2. Examples of Phenoxyimine Compounds Which Display Keto–Amine Solid State Structures<sup>25</sup>



of an available H-bonding interaction. This half of the molecule has bond lengths very similar to other phenoxyimines.<sup>25</sup> The naphthalene core and the two imine groups all lie in the same plane, however the *N*-aryl groups both lie orthogonal to the naphthalene core likely due to the unfavorable nonbonded interactions between the hydroxyl groups and the bulky isopropyl groups.

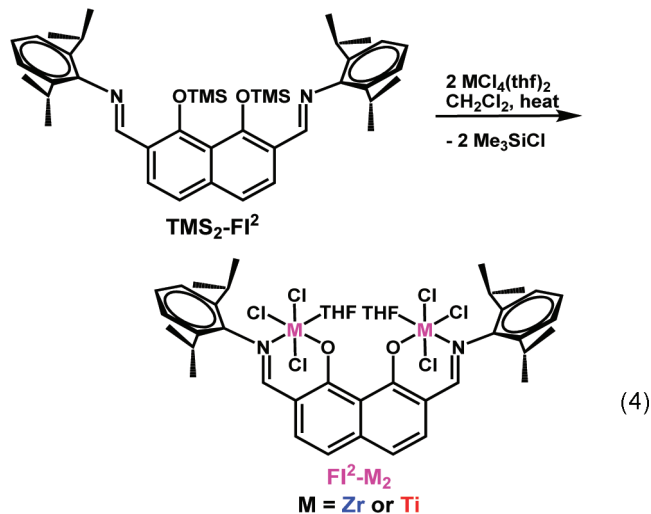
**III. Synthesis and Characterization of Binucleating Phenoxyimine Ligand Precursor 2,7-Di(2,6-diisopropylphenyl)imino-1,8-di(trimethylsiloxy)naphthalene (TMS<sub>2</sub>-FI<sup>2</sup>).** Similar to the reported chemistry of mononuclear phenoxyiminato ligands,<sup>9</sup> reactions of H<sub>2</sub>-FI<sup>2</sup> or Li<sub>2</sub>-FI<sup>2</sup> with group 4 metal synthons led to inseparable mixtures of products. In order to improve selectivity in the group 4 metalation reactions, the silylated derivative TMS<sub>2</sub>-FI<sup>2</sup> was synthesized by LiCH<sub>2</sub>TMS deprotonation and subsequent addition of trimethylchlorosilane (eq 3). In contrast to procedures reported for mononucleating phenoxyiminato ligands,<sup>9a</sup> heating is not required for complete silylation, and, in our hands, heating decomposes the ligand solutions to form unidentified products. The <sup>1</sup>H NMR spectral characteristics of TMS<sub>2</sub>-FI<sup>2</sup> show that the molecule adopts a symmetric geometry as expected due to the introduction of non-H-bonding, bulky trimethylsilyl groups which displace the *N*-aryl substituents furthest away from the central naphthalene core. The molecular structure of TMS<sub>2</sub>-FI<sup>2</sup> is confirmed by a single crystal X-ray structure determination (see Figure 3 below). It will be seen that clean group 4 metalations (*vide infra*) are readily accomplished with this reagent.



**IV. Molecular Structure of Compound TMS<sub>2</sub>-FI<sup>2</sup>.** A summary of crystal structure data for TMS<sub>2</sub>-FI<sup>2</sup> is presented in Table S1 in the Supporting Information, selected bond distances and angles are summarized in Table S3 in the Supporting Information, and a drawing is shown in Figure 3. Similar to the structure of H<sub>2</sub>-FI<sup>2</sup>, TMS<sub>2</sub>-FI<sup>2</sup> is planar, however the *N*-aryl groups are orthogonal to the naphthalene plane, and one trimethylsilyl group is located on either side of the naphthalene plane. The keto–amine metrical parameters observed in H<sub>2</sub>-

FI<sup>2</sup> are not evident in TMS<sub>2</sub>-FI<sup>2</sup>, and all bonds and angles are similar to those in more typical phenoxyimine compounds.<sup>25</sup> The lack of intramolecular H-bonding interactions and the bulky nature of the *N*-aryl and trimethylsilyl groups forces the imine groups to rotate away from the center of the naphthalene core.

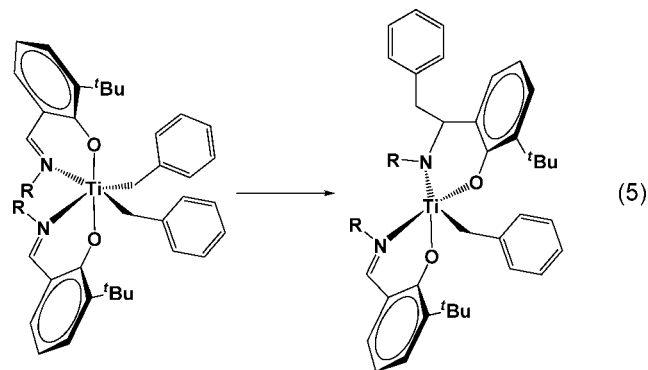
**V. Synthesis and Characterization of Bimetallic Phenoxyiminato Group 4 Complexes {1,8-(O)<sub>2</sub>C<sub>10</sub>H<sub>4</sub>-2,7-[CH=N(2,6-<sup>1</sup>Pr<sub>2</sub>C<sub>6</sub>H<sub>3</sub>)<sub>2</sub>]Zr<sub>2</sub>Cl<sub>6</sub>(THF)<sub>2</sub> (FI<sup>2</sup>-Zr<sub>2</sub>) and {1,8-(O)<sub>2</sub>C<sub>10</sub>H<sub>4</sub>-2,7-[CH=N(2,6-<sup>1</sup>Pr<sub>2</sub>C<sub>6</sub>H<sub>3</sub>)<sub>2</sub>]Ti<sub>2</sub>Cl<sub>6</sub>(THF)<sub>2</sub> (FI<sup>2</sup>-Ti<sub>2</sub>).** General methodologies for selectively synthesizing monophenoxyiminato group 4 complexes have been reported by several groups.<sup>9</sup> Selective addition of a *single phenoxyiminato ligand* to a group 4 metal precursor is best achieved using the trimethylsilyloxy derivative of the phenoxyimine ligand and the bis-THF adduct of appropriate the group 4 metal chloride.<sup>9</sup> In this way, clean double-metalation of both phenoxyimine functionalities of the FI<sup>2</sup> ligand is accomplished by addition of ZrCl<sub>4</sub>(THF)<sub>2</sub> at low temperature, followed by gradual increase in temperature to reflux for 24 h (eq 4). The reaction progress can be followed by monitoring the evolution of trimethylchlorosilane in the <sup>1</sup>H NMR spectrum. In the <sup>1</sup>H NMR spectrum, a large displacement of the imine proton resonance from δ ~ 8.8 ppm in TMS<sub>2</sub>-FI<sup>2</sup> to ~13.0 ppm in FI<sup>2</sup>-Zr<sub>2</sub> is indicative of Zr coordination. Analytically pure product may be obtained by recrystallization from a mixture of dichloromethane and toluene at -10 °C (see Supporting Information for details). Since X-ray quality single crystal growth attempts were unsuccessful, the bimetallic constitution was unambiguously verified by MALDI-TOF MS and elemental analysis. The elemental analysis is consistent with one THF ligand bound to each quasi-octahedral Zr center, in agreement with the MALDI-TOF data indicating that the THF ligands remain bound when the complex is ionized.



In a procedure similar to the synthesis of FI<sup>2</sup>-Zr<sub>2</sub>, FI<sup>2</sup>-Ti<sub>2</sub> was synthesized via the same basic trimethylchlorosilane elimination reaction (eq 4).<sup>9</sup> However, in contrast to the synthesis of FI<sup>2</sup>-Zr<sub>2</sub>, complete evolution of trimethylchlorosilane occurs in only 30 min of reflux for M = Ti, as compared to the 24 h required for FI<sup>2</sup>-Zr<sub>2</sub>. Analytically pure product is obtained by recrystallization from a mixture of dichloromethane and diethyl ether. Attempts to isolate X-ray quality single crystals were unsuccessful. However, unambiguous characterization using NMR spectroscopy, elemental analysis, and MALDI-TOF MS confirm the bimetallic constitution. The elemental analysis is in agreement with one THF ligand being bound to each quasi-octahedral Ti center. The MALDI mass spectrum indicates facile loss of both THF ligands with the major peak appearing at *m/z* = 844.8, which corresponds to the mass of FI<sup>2</sup>-Ti<sub>2</sub> minus the

mass of two THF molecules. The  $^1\text{H}$  NMR spectrum of  $\text{FI}^2\text{-Ti}_2$  indicates a shift of the imine proton resonance from  $\delta$  8.8 to 13.1 ppm on coordination of Ti and elimination of trimethylchlorosilane. As in the case of  $\text{FI}^2\text{-Zr}_2$ , this is consistent with Ti coordination to N. Attempts to prepare analogous complexes via either alkane or amine elimination reactions using the corresponding group 4 homoleptic alkyls or amides and  $\text{H}_2\text{-FI}^2$  did not afford clean reactions.

**VI. Polymerization Properties of Bimetallic Complexes  $\text{FI}^2\text{-Zr}_2$  and  $\text{FI}^2\text{-Ti}_2$  Activated with MAO.** Activation of  $\text{FI}^2\text{-Zr}_2$  and  $\text{FI}^2\text{-Ti}_2$  is achieved by vigorously shaking these compounds with a solution of MAO in toluene for 30 min. These complexes alone are insoluble in toluene, however they are readily dissolved and activated under these reaction conditions. The polymerization studies were limited to using MAO as the cocatalyst since neither benzyl nor methyl derivatives of  $\text{FI}^2\text{-Zr}_2$  and  $\text{FI}^2\text{-Ti}_2$  could be obtained cleanly. Group 4 mono- and bis(phenoxyiminato)alkyls are prone to decomposition by several identified pathways, including ligand redistribution and nucleophilic attack on the imine carbon center to form phenoxyamides. Phenoxyiminato group 4 complexes bearing methyl or benzyl ligands are known to undergo reaction by either intermolecular or intramolecular pathways to convert the imine functionality to an amido group (eq 5).<sup>26</sup> Monophenoxyiminato group 4 complexes are also reported to undergo disproportionation (eq 6).<sup>9a,27</sup> In the present study, other methods of precatalyst activation, such as *in situ* addition of  $\text{Al}^i\text{Bu}_3$ , followed by  $\text{Ph}_3\text{C}^+\text{B}(\text{C}_6\text{F}_5)_4^-$ ,<sup>10b</sup> afforded very low polymerization activity.



FI = phenoxyimine

M = Ti, Zr

**A. Ethylene Homopolymerization Studies.** Ethylene homopolymerizations were carried out under conditions identical<sup>28</sup> to those previously reported for CGC catalysts  $\text{Zr}_2$  and  $\text{Ti}_2$ .<sup>5</sup> The activities for  $\text{FI}^2\text{-Ti}_2$  are modest and are slightly lower than those of  $\text{FI}^2\text{-Zr}_2$  (Table 1, entry 6 versus 2). However, at 40 °C,  $\text{FI}^2\text{-Zr}_2$  produces polyethylene with an activity  $\sim 6.4\times$  that of mononuclear  $\text{FI-Zr}_1$ , and  $\text{FI}^2\text{-Ti}_2$  produces polyethylene with an activity  $\sim 1.9\times$  that of mononuclear  $\text{FI-Ti}_1$ . As reported for other mononuclear phenoxyiminato catalysts,<sup>9c,d</sup>  $\text{FI-Zr}_1$  and  $\text{FI-Ti}_1$  produce linear, high  $M_w$  polyethylenes, however the substantial polydispersities indicate that multiple catalytic sites or conformations may be involved. The binuclear complexes  $\text{FI}^2\text{-Zr}_2$  and  $\text{FI}^2\text{-Ti}_2$  also produce very high molecular weight linear polyethylenes at 24 °C, as indicated by the insolubility of the polymeric products. However, increasing the polymerization temperature to 40 °C lowers the product  $M_w$  to  $\sim 155\,000$  g/mol for  $\text{FI}^2\text{-Zr}_2$ -mediated polymerizations. For  $\text{FI}^2\text{-Ti}_2$ -mediated polymerizations at 40 °C, the polyethylene  $M_w$  is

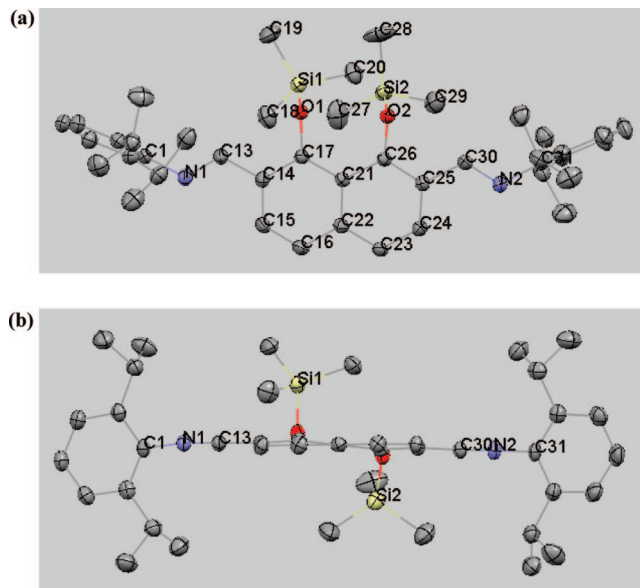


**Figure 3.** Molecular structure and atom numbering scheme for 2,7-di(2,6-diisopropylphenyl)imino-1,8-di(trimethylsiloxy)naphthalene ( $\text{TMS}_2\text{-FI}^2$ ). Thermal ellipsoids are drawn at the 50% probability level: (a) top view of naphthyl skeleton and (b) side view of the naphthyl plane. Selected bond distances (Å) include: C17–O1 = 1.370(1), O1–Si1 = 1.6822(15), C26–O2 = 1.361(2), C13–N1 = 1.274(3), C30–N2 = 1.262(3).

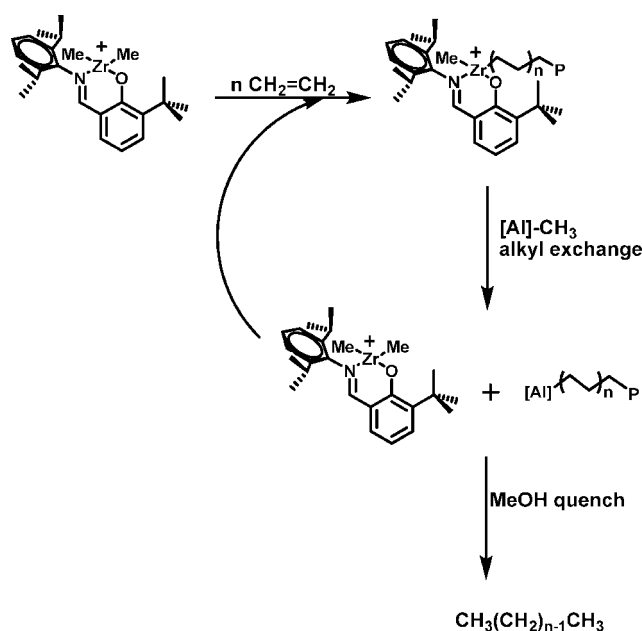
lowered to  $\sim 297\,000$  g/mol, slightly lower than the polyethylene derived from  $\text{FI-Ti}_1$  under the same conditions (entry 7 vs 8). GPC-derived polydispersities are, however, somewhat greater than 2.0 suggesting that multiple active sites or conformations may be present during the polymerization process. As previously reported, broadened polyethylene polydispersities are commonly observed with phenoxyiminato polymerization catalysts.<sup>29</sup> The melting points of the ethylene homopolymers were determined by DSC, and the values are indicative of linear polyethylenes. The ethylene homopolymers were also analyzed by  $^1\text{H}$  and  $^{13}\text{C}$  NMR spectroscopy which further indicates that the polymers are linear polyethylenes with no detectable branching.  $^1\text{H}$  NMR spectral integrals indicate an approximate ratio of vinylic endgroups to saturated endgroups of  $\sim 1:8$ . Saturated endgroups suggest that the termination pathway is chain transfer to Al (e.g., Scheme 3),<sup>30</sup> while vinylic endgroups indicate  $\beta$ -hydride elimination (either to metal or to monomer).<sup>3–5</sup> Chain transfer to Al has been identified as the major chain transfer pathway for a bis-phenoxyiminato zirconium catalyst in ethylene homopolymerization.<sup>31</sup> In the present case, a 1:8 ratio of unsaturated to saturated endgroups corresponds to approximately 68% chain transfer to Al and 32%  $\beta$ -hydride elimination since every polyethylene chain terminated by chain transfer to Al would have two methyl endgroups, and every polyethylene chain terminated by  $\beta$ -hydride elimination would have one methyl and one vinyl endgroup.

**B. Ethylene +  $\alpha$ -Olefin Copolymerization Studies.** Ethylene + 1-hexene and ethylene + 1-octene copolymerization data are presented in Table 1. As observed in the ethylene homopolymerizations (*vide supra*), the activities of  $\text{FI}^2\text{-Ti}_2$  are again slightly lower than those of  $\text{FI}^2\text{-Zr}_2$  for both ethylene + 1-hexene (Table 1, entry 10 vs 12) and ethylene + 1-octene copolymerizations (Table 1, entry 6 vs 8). However, the activity of  $\text{FI}^2\text{-Ti}_2$  for both of these copolymerizations is nearly  $2\times$  that of  $\text{FI-Ti}_1$  under identical reaction conditions (Table 1, entries 7 vs 8 and 9 vs 10). While  $\text{FI-Zr}_1$  exhibits extremely low activity for ethylene + 1-hexene copolymerizations and ethylene + 1-octene copolymerizations, note that  $\text{FI}^2\text{-Zr}_2$  is  $12\times$  more active than  $\text{FI-Zr}_1$  for ethylene + 1-hexene copolymerization (Table

**Table 1. Ethylene Homopolymerization and Ethylene +  $\alpha$ -Olefin Copolymerization Results for Catalysts FI-Zr<sub>1</sub>, FI<sup>2</sup>-Zr<sub>2</sub>, FI-Ti<sub>1</sub>, and FI<sup>2</sup>-Ti<sub>2</sub><sup>a</sup>**

entry	catalyst	comonomer	temp (°C)	comonomer concn (M)	polymer yield (g)	activity <sup>b</sup> ( $\times 10^3$ )	T <sub>m</sub> (°C) <sup>c</sup>	10 <sup>3</sup> M <sub>w</sub> <sup>d</sup>	M <sub>w</sub> /M <sub>n</sub> <sup>d</sup>	comonomer incorporation (%) <sup>c</sup>
1	FI-Zr <sub>1</sub>	n/a	24	n/a	0.019	2.1	131.8	too insol.	too insol.	n/a
2	FI <sup>2</sup> -Zr <sub>2</sub>	n/a	24	n/a	0.167	16	142.6	too insol.	too insol.	n/a
3	FI-Zr <sub>1</sub>	n/a	40	n/a	0.036	3.6	130.3	too insol.	too insol.	n/a
4	FI <sup>2</sup> -Zr <sub>2</sub>	n/a	40	n/a	0.230	23	140.4	155	3.92	n/a
5	FI-Ti <sub>1</sub>	n/a	24	n/a	0.025	2.5	135.9	675	23.7	n/a
6	FI <sup>2</sup> -Ti <sub>2</sub>	n/a	24	n/a	0.053	5.3	136.3	too insol.	too insol.	n/a
7	FI-Ti <sub>1</sub>	n/a	40	n/a	0.043	4.3	134.8	315	6.55	n/a
8	FI <sup>2</sup> -Ti <sub>2</sub>	n/a	40	n/a	0.082	8.3	135.8	297	4.49	n/a
9	FI-Zr <sub>1</sub>	1-octene	40	0.72	0.022	2.2	128.5	22	11.9	4.1
10	FI <sup>2</sup> -Zr <sub>2</sub>	1-octene	40	0.72	0.083	8.3	125.6	105	3.61	7.3
11	FI-Ti <sub>1</sub>	1-octene	40	0.72	0.022	2.2	120.3	96	5.46	8.4
12	FI <sup>2</sup> -Ti <sub>2</sub>	1-octene	40	0.72	0.039	3.9	121.7	182	3.33	15.2
13	FI-Ti <sub>1</sub>	1-hexene	40	0.72	0.027	2.7	128.6	188	33.6	4.3
14	FI <sup>2</sup> -Ti <sub>2</sub>	1-hexene	40	0.72	0.045	4.5	120.6	76	3.91	9.4
15	FI-Zr <sub>1</sub>	1-hexene	40	0.72	0.015	1.0	125.0	21	9.61	7.4
16	FI <sup>2</sup> -Zr <sub>2</sub>	1-hexene	40	0.72	0.150	12	125.8	98	3.31	11.0

<sup>a</sup> (Co)polymerizations carried out on a high-vacuum line with 10  $\mu$ mol Ti/Zr and MAO as cocatalyst (Al:M<sup>+</sup> = 1000:1) in 50 mL of toluene under 1.0 atm of ethylene pressure for 60 to 90 min. <sup>b</sup> Gram polymer/[mol M<sup>+</sup> · atm · h]. <sup>c</sup> From GPC vs polystyrene standards. <sup>d</sup> Comonomer incorporation calculated from the <sup>13</sup>C NMR spectra.<sup>40</sup> n/a = not applicable.

**Scheme 3. Chain Transfer to Aluminum as a Termination Pathway for Ethylene Polymerization**

1, entry 15 vs 16) and nearly 3 $\times$  more active than FI-Zr<sub>1</sub> for ethylene + 1-octene copolymerization (Table 1, entry 10 vs 9). In regard to selectivity for comonomer enchainment, the selectivity of FI<sup>2</sup>-Ti<sub>2</sub> for 1-hexene incorporation is 4.5 $\times$  that of FI<sup>2</sup>-Zr<sub>2</sub> (Table 1, entry 10 vs 11), and 2.2 $\times$  that of FI-Ti<sub>1</sub> (Table 1, entry 10 vs 9). The selectivity of FI<sup>2</sup>-Zr<sub>2</sub> for 1-hexene incorporation is 1.5 $\times$  that of FI-Zr<sub>1</sub> (Table 1, entry 16 vs 15). The selectivity of FI<sup>2</sup>-Ti<sub>2</sub> for 1-octene incorporation is 1.8 $\times$  that of FI-Ti<sub>1</sub> (Table 1, entry 7 vs 8), and, interestingly, 2.1 $\times$  that of FI<sup>2</sup>-Zr<sub>2</sub> (Table 1, entry 8 vs 6). The selectivity for 1-octene incorporation by FI<sup>2</sup>-Zr<sub>2</sub> is 1.8 $\times$  that of FI-Zr<sub>1</sub> (Table 1, entry 6 versus entry 5). Maximum comonomer incorporation densities are achieved by the Ti catalysts, with 1-octene levels as high as 15.2% achieved for FI<sup>2</sup>-Ti<sub>2</sub>. For ethylene + 1-hexene copolymerizations mediated by FI<sup>2</sup>-Zr<sub>2</sub>, the copolymer M<sub>w</sub> of the copolymer is  $\sim$ 4.7 $\times$  greater than that mediated by FI-Zr<sub>1</sub>, however, for those mediated by FI<sup>2</sup>-Ti<sub>2</sub>, M<sub>w</sub> is nearly half-that of FI-Ti<sub>1</sub>. For the ethylene + 1-octene copolymerizations mediated by FI<sup>2</sup>-Zr<sub>2</sub>, the M<sub>w</sub> is  $\sim$ 5 $\times$  than in the same copolymerizations mediated by FI-Zr<sub>1</sub>. The same trend also

holds for the 1-octene copolymerization using FI<sup>2</sup>-Ti<sub>2</sub>, although the M<sub>w</sub> is only  $\sim$ 2 $\times$  greater than that of the copolymer obtained using FI-Ti<sub>1</sub> as catalyst. In all but one case, the PDIs of the polymers derived from binuclear catalysts are narrower than those derived from the mononuclear catalysts. Vinylic endgroups are detected in the <sup>1</sup>H NMR spectra of these copolymers, however accurate determination of the ratio of vinylic to saturated endgroups is not possible due to an overlap of the signals from endgroup methyl groups and butyl branch methyl groups.

*C. Ethylene + Methylene-cyclopentane (MCP) and Ethylene + Methylene-cyclohexane (MCH) Copolymerization Studies.* Ethylene + MCP and ethylene + MCH copolymerization data are presented in Table 2. With MCP as the solvent, MCP is incorporated using the FI-Ti<sub>1</sub> and FI<sup>2</sup>-Ti<sub>2</sub> catalysts at low levels and with moderate polymerization activity. In contrast, FI<sup>2</sup>-Ti<sub>2</sub> is  $\sim$ 4.5 $\times$  more active and the copolymer M<sub>w</sub> is  $\sim$ 2 $\times$  greater than the copolymers obtained using FI-Ti<sub>1</sub> as the catalyst. The low selectivity for comonomer incorporation for both FI-Ti<sub>1</sub> and FI<sup>2</sup>-Ti<sub>2</sub> catalysts (<1%) indicates a substantial barrier for MCP insertion. This result is in marked contrast to the ethylene + MCH copolymerizations. Under identical reaction conditions, MCH is incorporated to a much greater extent for both FI-Ti<sub>1</sub> (3.4%) and FI<sup>2</sup>-Ti<sub>2</sub> (11.6%) catalyzed copolymerization. Note also that FI<sup>2</sup>-Ti<sub>2</sub> incorporates  $\sim$ 3.4 $\times$  more MCH than does FI-Ti<sub>1</sub> (Table 2, entry 4 vs 3), and that M<sub>w</sub> is  $\sim$ 5 $\times$  greater for the FI<sup>2</sup>-Ti<sub>2</sub>-derived copolymer than for the copolymer obtained with FI-Ti<sub>1</sub>. The <sup>1</sup>H and <sup>13</sup>C NMR spectra of the copolymers indicate that MCP and MCH are incorporated via ring-unopened pathways,<sup>14a</sup> and the integral ratio of vinylic endgroups to saturated endgroups ( $\sim$ 1:7) indicates  $\sim$ 65% chain transfer to Al and 35%  $\beta$ -hydride elimination.

It is presumed that the proximate metal center assists in the insertion of comonomers (see more in the Discussion section), and it is likely that the additional methylene group and greater skeletal flexibility of MCH versus MCP, plays a role in the enhanced comonomer enchainment. Specifically, the geometry of the catalyst/comonomer combination may be more ideal for insertion of MCH than for MCP. Interestingly, in contrast, the catalysts FI-Zr<sub>1</sub> and FI<sup>2</sup>-Zr<sub>2</sub> do not incorporate measurable quantities of MCP or MCH under the same polymerization conditions. In fact, polyethylene homopolymer is obtained under these conditions, indicating a marked metal center dependency

Table 2. Ethylene + MCA and Ethylene +  $\alpha,\omega$ -Diene Copolymerization Results for FI-Ti<sub>1</sub>, FI<sup>2</sup>-Ti<sub>2</sub>, FI-Zr<sub>1</sub>, and FI<sup>2</sup>-Zr<sub>2</sub> Catalysts<sup>a</sup>

entry	cat	comonomer	comonomer concn (M)	polymer yield (g)	activity ( $\times 10^3$ ) <sup>b</sup>	T <sub>m</sub> (°C) <sup>c</sup>	10 <sup>3</sup> M <sub>w</sub> <sup>d</sup>	M <sub>w</sub> /M <sub>n</sub> <sup>d</sup>	comonomer incorporation (%) <sup>e</sup>	cis/trans
1	FI-Ti <sub>1</sub>	MCP	neat	0.025	3.4	128.3	58	20.2	0.4	n/a
2	FI <sup>2</sup> -Ti <sub>2</sub>	MCP	neat	0.115	15	126.4	121	4.01	0.7	n/a
3	FI-Ti <sub>1</sub>	MCH	neat	0.080	8.1	124.3	20	13.1	3.4	n/a
4	FI <sup>2</sup> -Ti <sub>2</sub>	MCH	neat	0.096	9.7	124.7	104	3.48	11.6	n/a
5	FI-Zr <sub>1</sub>	MCP	neat	0.042	3.3	135.3	n/a	n/a	PE	n/a
6	FI <sup>2</sup> -Zr <sub>2</sub>	MCP	neat	0.026	6.9	134.2	n/a	n/a	PE	n/a
7	FI-Zr <sub>1</sub>	MCH	neat	0.031	2.6	130.5	n/a	n/a	PE	n/a
8	FI <sup>2</sup> -Zr <sub>2</sub>	MCH	neat	0.077	6.2	137.9	n/a	n/a	PE	n/a
9	FI-Zr <sub>1</sub>	1,5-HD	0.3	0.012	1.0	127.9	34	10.3	7.9	44/56
10	FI <sup>2</sup> -Zr <sub>2</sub>	1,5-HD	0.3	0.151	15	131.5	78	3.22	10.3	60/40
11	FI-Zr <sub>1</sub>	1,4-PD	0.3	0.292	29	124.0	73	3.28	2.1	82/18
12	FI <sup>2</sup> -Zr <sub>2</sub>	1,4-PD	0.3	0.742	74	124.0	75	4.81	5.4	69/31
13	FI-Ti <sub>1</sub>	1,5-HD	0.3	0.004	0.3	123.8	n/a	n/a	n/a	n/a
14	FI <sup>2</sup> -Ti <sub>2</sub>	1,5-HD	0.3	0.003	0.2	122.6	n/a	n/a	n/a	n/a
15	FI-Ti <sub>1</sub>	1,4-PD	0.3	0.008	0.8	123.4	n/a	n/a	n/a	n/a
16	FI <sup>2</sup> -Ti <sub>2</sub>	1,4-PD	0.3	0.007	0.7	121.4	n/a	n/a	n/a	n/a

<sup>a</sup> Copolymerizations carried out at room temperature on a high-vacuum line with 10  $\mu$ mol Ti/Zr and MAO as cocatalyst (Al:M<sup>+</sup> = 1000:1) under 1.0 atm ethylene pressure. Copolymerizations carried out for 45–75 min. <sup>b</sup> Gram polymer/[(mol M<sup>+</sup>) $\cdot$ atm $\cdot$ h]. <sup>c</sup> By DSC. <sup>d</sup> From GPC vs polystyrene standards. <sup>e</sup> Comonomer incorporations from <sup>13</sup>C NMR spectra. <sup>14a,21a,41</sup> PE = polyethylene (as judged by <sup>13</sup>C NMR spectroscopy and DSC); n/a = not applicable.

of the comonomer enchainment selectivity in these types of catalysts.

*D. Ethylene + 1,5-HD and Ethylene + 1,4-PD Copolymerization Studies.* Ethylene + 1,5-HD and ethylene + 1,4-PD copolymerization data are presented in Table 2. In marked contrast to the MCA copolymerizations, FI-Zr<sub>1</sub> and FI<sup>2</sup>-Zr<sub>2</sub> perform far more efficiently than do FI-Ti<sub>1</sub> and FI<sup>2</sup>-Ti<sub>2</sub> in these copolymerizations. For significantly more dilute comonomer concentrations (0.30 M) than employed in the MCA copolymerizations above, 1,5-HD is copolymerized with good incorporation levels (10.3%) and moderate activity using FI<sup>2</sup>-Zr<sub>2</sub> as the catalyst. Compared to the FI-Zr<sub>1</sub>-derived ethylene + 1,5-HD copolymer, FI<sup>2</sup>-Zr<sub>2</sub> enchains 1.3 $\times$  (Table 2, entry 10 vs 9) more 1,5-HD at an activity which is 15.3 $\times$  greater than FI-Zr<sub>1</sub>. The M<sub>w</sub> of the FI<sup>2</sup>-Zr<sub>2</sub>-derived copolymer (78 000 g/mol, PDI = 3.22) is 2.3 $\times$  greater than the M<sub>w</sub> of the FI-Zr<sub>1</sub>-derived copolymer (34 000 g/mol, PDI = 10.3), and the PDI is much narrower for the FI<sup>2</sup>-Zr<sub>2</sub>-derived copolymer. In the polymerization process, both FI<sup>2</sup>-Zr<sub>2</sub> and FI-Zr<sub>1</sub> convert all 1,5-HD units into a mixture of enchainment *cis*- and *trans*-1,3-cyclopentyl fragments (structure C) according to the <sup>13</sup>C NMR spectra of the copolymers.<sup>20,21</sup> No signals associated with cross-links are detected in the NMR spectra, however vinylic endgroups ( $\delta$  5.1 ppm) and a very small amount of pendant vinylic groups ( $\delta$  5.5 ppm) are observed in the <sup>1</sup>H NMR spectra of the copolymers. An approximate ratio of 1:5 was observed for unsaturated to saturated endgroups, corresponding to  $\sim$ 54% chain transfer to Al and 46%  $\beta$ -hydride elimination. The FI<sup>2</sup>-Zr<sub>2</sub>-derived copolymer consists of 60% *cis*- and 40% *trans*-1,3-cyclopentyl fragments, while the FI-Zr<sub>1</sub>-derived copolymer consists of 44% *cis*- and 56% *trans*-1,3-cyclopentyl fragments according to the <sup>13</sup>C NMR spectroscopic assay.<sup>20,21</sup> A plausible explanation for this selectivity difference is presented in the Discussion section.

Ethylene + 1,4-PD copolymerizations proceed with good comonomer incorporation levels and moderate activities using both FI-Zr<sub>1</sub> and FI<sup>2</sup>-Zr<sub>2</sub> catalyst systems. FI<sup>2</sup>-Zr<sub>2</sub> turns over with an activity  $\sim$ 2.5 $\times$  greater than does FI-Zr<sub>1</sub>, and the 1,4-PD comonomer is incorporated to  $\sim$ 2.6 $\times$  greater density using FI<sup>2</sup>-Zr<sub>2</sub> as compared to FI-Zr<sub>1</sub> (Table 2, entry 12 vs 11). The GPC-derived M<sub>w</sub> of the FI<sup>2</sup>-Zr<sub>2</sub>-derived copolymer (75 000 g/mol, PDI = 4.81) is nearly the same as the FI-Zr<sub>1</sub>-derived copolymer (73 000 g/mol, PDI = 3.28). According to the <sup>13</sup>C NMR spectra of the copolymers,<sup>21</sup> all 1,4-PD units are converted to a mixture of *cis*- and *trans*-1,3-cyclohexyl fragments. No signals associated with cross-links are detected in the NMR

spectra, however vinylic endgroups ( $\delta$  5.1 ppm) and a small amount of pendant vinylic groups ( $\delta$  5.5 ppm) are observed in the <sup>1</sup>H NMR spectra of the copolymers. As in the ethylene + 1,5-HD copolymers, an approximate ratio of 1:5 was observed for unsaturated to saturated endgroups, corresponding to  $\sim$ 54% chain transfer to Al and 46%  $\beta$ -hydride elimination. The FI<sup>2</sup>-Zr<sub>2</sub>-derived copolymer consists of 69% *cis*- and 31% *trans*-1,3-cyclohexyl fragments, and the FI-Zr<sub>1</sub>-derived copolymer consists of 82% *cis*- and 18% *trans*-1,3-cyclopentyl fragments according to the <sup>13</sup>C NMR spectra of the copolymers. Under identical reaction conditions, FI-Ti<sub>1</sub> and FI<sup>2</sup>-Ti<sub>2</sub> produce less than 10 mg of copolymer in these ethylene +  $\alpha,\omega$ -diene copolymerizations.

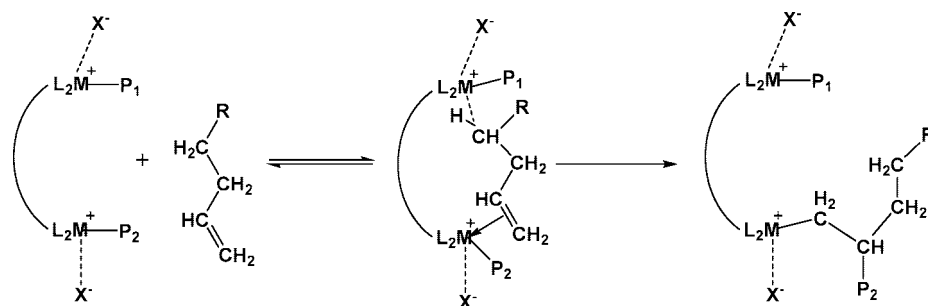
## Discussion

In the case of the binuclear CGCs (Chart 1), it was proposed that when the olefinic unit of an alkene comonomer binds to one metal center, the second highly electrophilic d<sup>0</sup> center can engage in secondary, possibly agostic interactions,<sup>32</sup> leading to enhanced comonomer binding affinity/activating capacity, thereby modifying relative enchainment and chain transfer rates (structure I and Scheme 4).

Density functional theory (DFT/B3LYP) calculations on C1-Zr<sub>2</sub> show that the agostic interaction contributes  $\sim$ 2 kcal/mol stabilization to the coordinated bimetallic  $\alpha$ -olefin complex in which the alkyl chain is proximate to the adjacent metal center (Figure 4).<sup>33</sup> It is found that the C7–H bond in structure II<sup>35</sup> is elongated by  $\sim$ 0.02 Å, and the effective charge on Zr2 in structure II (+1.83) is substantially lower than that of Zr2 in structure III (+1.93), further indicating an agostic interaction with Zr2. This agostic stabilization is reasonably associated with the selectivity for olefin comonomer enchainment which is observed for bimetallic catalysts relative to their mononuclear analogues. Therefore, introducing rigid ligation and contracting the distance between metal centers should favor cooperative enchainment processes. The next important issue is whether and how these binuclear enchainment effects are operative in the present family of binuclear phenoxyiminato catalysts, how they vary with group 4 metal, and whether the comonomer scope can be broadened.

The results of the present investigation indicate that as the nuclearity of the phenoxyiminato group 4 catalysts is increased, polymerization properties are dramatically altered both in terms of activity as well as selectivity for bulky olefinic comonomer incorporation. Overall productivities are significantly increased

Scheme 4. Proposed Scenario for Enhanced Comonomer Enchainment by Bimetallic Group 4 Catalysts



in all cases for the binuclear versus the mononuclear catalysts, indicating enhanced rates of not only ethylene homopolymerization but also of comonomer enchainment relative to ethylene enchainment. In previous studies of binuclear CGC-based catalysts, olefinic comonomers were observed to depress polymerization activity, presumably due to competition for coordination sites, although selectivities for comonomer incorporation were substantially greater than for mononuclear CGC catalysts.<sup>5,13</sup> In the sections that follow, we discuss the likely origins of these effects and the polymers produced.

**I. Structural Design Considerations for Ligand FI<sup>2</sup>.** When we set out to synthesize a new family of binuclear transition metal catalysts, we sought to maximize the potential for metal–metal cooperativity during polymerization while using metal–ligand sets conducive to rapid olefin activation and enchainment. The first characteristic to modify versus earlier **Ti<sub>2</sub>**, **Zr<sub>2</sub>**, **C1-Ti<sub>2</sub>**, and **C1-Zr<sub>2</sub>** CGC structures was the positional rigidity of the metal centers. A rigid ligand structure would prevent the metal centers from rotating away from each other as is possible in **C1-Ti<sub>2</sub>** and **Ti<sub>2</sub>** (Chart 1). While **Ti<sub>2</sub>** has a negligible barrier to rotation, **C1-Ti<sub>2</sub>** has an estimated barrier for 360° rotation of ~65 kcal/mol,<sup>3b</sup> but still possesses substantial conformational mobility. In contrast, the **FI<sup>2</sup>** ligand design ‘locks’ the metal centers such that they are always disposed with the shortest possible intermetal distance (5.4–5.9 Å estimated<sup>12</sup>). Whereas the catalytic centers in the **C1-Ti<sub>2</sub>** and **Ti<sub>2</sub>** CGCs may rotate in solution away from shortest estimated

**M···M** distances of ~6.0 Å and ~6.6 Å, respectively, the rigid naphthalene backbone prevents this type of rotation. Although the crystal structures of **FI<sup>2</sup>-Zr<sub>2</sub>** and **FI<sup>2</sup>-Ti<sub>2</sub>** are not available, the molecular structures can be estimated to be near-planar with respect to the naphthalene core and the metal centers, with a metal–metal distance estimated to be 5.4 to 5.9 Å.<sup>12</sup> We introduced *o,o'* solubilizing groups on the *N*-aryl substituents in order to maintain good solubility. The ligand structure chosen is similar to two ligands reported by Glaser in multinucleating Cu systems designed for applications as magnetic materials (Figure 4).<sup>34</sup> The reported Cu complexes were characterized by single-crystal XRD, and in some cases, the structures are planar with respect to the metal centers and the naphthyl moiety.

**II. Ethylene Homopolymerizations.** Bochmann reported that a series of monophenoxyiminato Zr and Ti complexes (Figure 5) produces very high *M<sub>w</sub>* linear polyethylenes when activated with MAO.<sup>9a,b</sup> When the polymerization experiments were carried out at 60 °C, *M<sub>w</sub>* was substantially decreased.<sup>9a</sup> These characteristics are also observed in the present study for both **FI<sup>2</sup>-Zr<sub>2</sub>** and **FI<sup>2</sup>-Ti<sub>2</sub>** activated with MAO. Under room temperature polymerization conditions, the polyethylene products are completely insoluble. However, at elevated polymerization temperatures (40 °C), product *M<sub>w</sub>*s are sufficiently depressed to obtain soluble polymers, informative NMR spectra, and good GPC traces, although the polydispersities are still somewhat greater than 2.0, suggesting multiple active sites or conformations. As previously mentioned, phenoxyiminato group 4

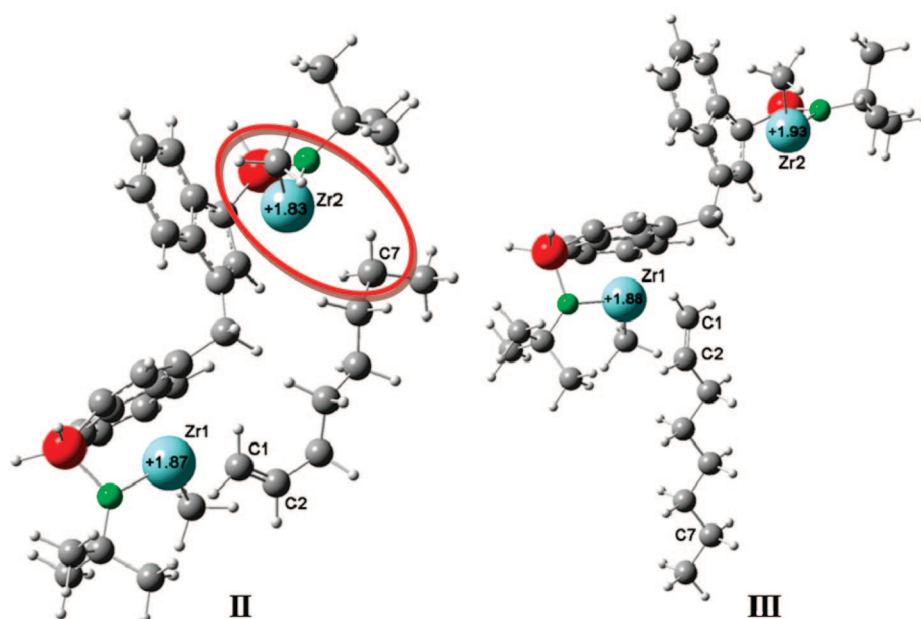


**Figure 4.** Density functional theory (DFT/B3LYP) results, which show that the  $\pi$ -complex of 1-octene with **C1-Zr<sub>2</sub>** in which the alkyl chain interacts with the proximate Zr-center (**II**) is more stable than if the alkyl chain is bent away from the proximate Zr-center (**III**). Diagram adapted from ref 35.

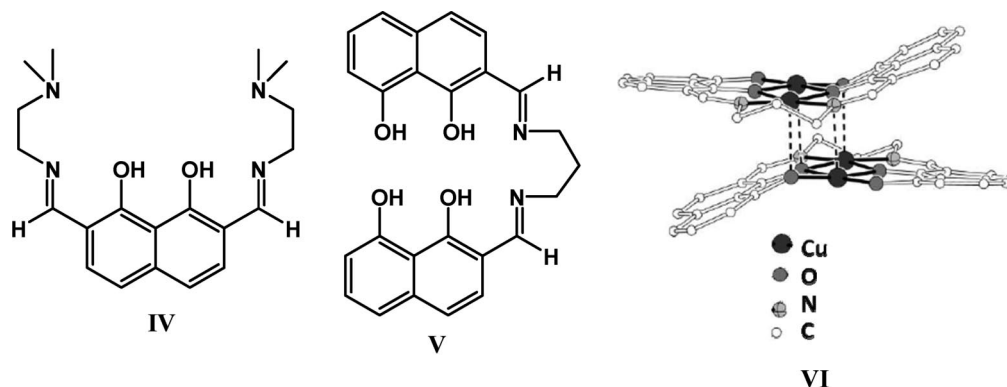
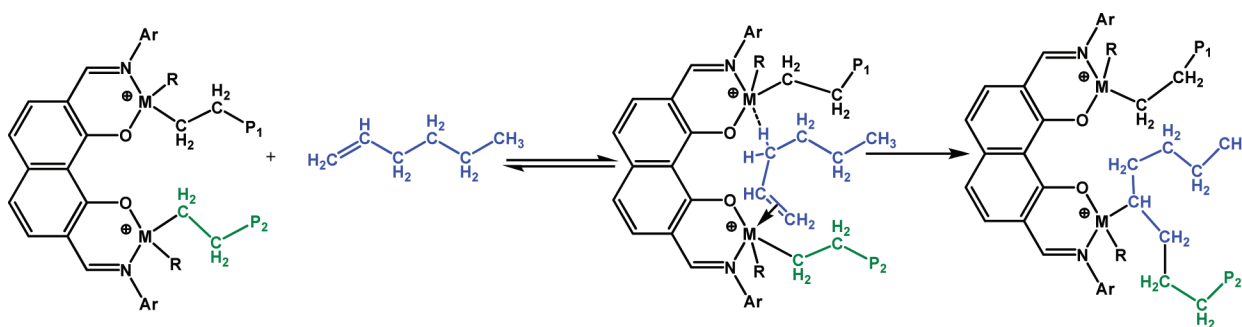


**Figure 5.** Multidentate ligands similar to  $H_2\text{-FI}^2$ . Structure **VI** shows an X-ray diffraction crystal structure of a **IV**-Cu complex, revealing that half of the ligand lies in the same plane as Cu.<sup>36</sup>

**Scheme 5. Proposed Scenario for Enhanced  $\alpha$ -Olefin Enchainment by Bimetallic Catalysts (M = Ti, Zr; Ar = 2,6-Diisopropylphenyl; R = Alkyl, H; Anion Omitted for Clarity)**

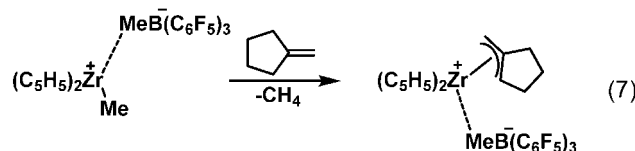


complexes are prone to alteration via ligand rearrangement processes and/or nucleophilic attack on the imine functionality, which could, in principle, create additional catalytic species.

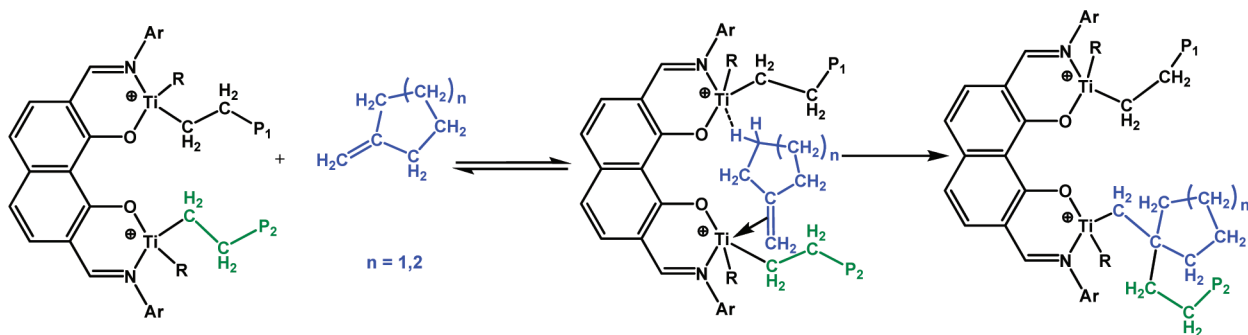
**III. Ethylene +  $\alpha$ -Olefin Copolymerizations.** Both the present ethylene + 1-hexene and ethylene + 1-octene copolymerization data indicate that, compared to typical experimental olefin polymerization conditions at low catalyst concentration levels ( $10^{-4}$ – $10^{-8}$  M), the close enforced contact between the two catalytic centers leads to significantly greater extents of comonomer enchainment. It is likely that coordination/activation of the  $\alpha$ -olefin to one cationic metal center is stabilized by a secondary, possibly agostic interaction with the proximate cationic metal center, which may facilitate/stabilize  $\alpha$ -olefin capture/binding at the metal center and enhance the subsequent enchainment probability (Scheme 5 and Figure 4). In the case of the binuclear versus mononuclear CGC catalysts, dramatic comonomer enchainment selectivity is observed along with substantial branching in ethylene homopolymerizations.<sup>5c,d,f,13</sup> However, *reduced* overall polymerization activities are observed for the binuclear CGC catalysts versus the mononuclear CGC analogues. For example, in ethylene + 1-octene copolymerizations with **Ti**<sub>2</sub> and **Ti**<sub>1</sub> as the catalysts and **B**<sub>1</sub> as the cocatalyst, **Ti**<sub>1</sub> produces copolymer with an activity which is 2× that of **Ti**<sub>2</sub>. It was postulated that this is possibly due to the  $\alpha$ -olefin partially blocking or competing for ethylene activation and enchainment sites.<sup>5f</sup> However, for the present phenoxyiminato catalysts in the current study, an enhancement in activity is observed, albeit modest in some cases. In this study, the bimetallic catalysts exhibit significantly greater activity than the monometallic complexes in *all* analogous cases (i.e., where the only experimental variable is monometallic vs bimetallic catalyst and reaction conditions are identical). We hypothesize that this is a result of cooperativity effects between the two activated catalyst centers during the polymerization which creates an advantageous coordination environment around the linked

catalysts, thereby increasing the enchainment efficiency during both ethylene homopolymerizations and ethylene + olefin copolymerizations.

**IV. Sterically Encumbered MCA Copolymerizations.** In accord with previous observations on CGCTi-mediated ethylene + MCA copolymerizations,<sup>14</sup> **MCP** and **MCH** are incorporated via ring-unopened pathways using **FI**<sup>2</sup>-**Ti**<sub>2</sub> and **FI**-**Ti**<sub>1</sub> as the catalysts to yield macromolecular products **C** and **D** (Chart 4). However, under identical reaction conditions, **FI**<sup>2</sup>-**Zr**<sub>2</sub> and **FI**-**Zr**<sub>1</sub> yield only ethylene homopolymer. The minimal ring strain energy associated with these comonomers likely has a strong influence on their enchainment pathways in that copolymerizations proceed without ring-opening, which is thermodynamically unfavorable. For comonomers **MCP** and **MCH**, different catalytic pathways are in principle accessible, depending on the particular group 4 catalyst. For example,  $(C_5H_5)_2ZrMe^+MeB(C_6F_5)_3^-$  reacts with **MCP** to form an  $\eta^3$ -allyl complex without enchainment (eq 7).<sup>35</sup> It was also reported that, with



$(C_5H_5)_2ZrMe^+MeB(C_6F_5)_3^-$  as the catalyst, **MCP** and **MCH** are ultimately converted to the thermodynamically favored internal olefins **A** and **B** (Chart 4), again without enchainment.<sup>14c</sup> The same isomerization reactions occur when CGCZr- $Me^+MeB(C_6F_5)_3^-$  catalysts are employed.<sup>14b</sup> While neither  $(C_5H_5)_2ZrMe^+MeB(C_6F_5)_3^-$  nor CGCZr $Me^+MeB(C_6F_5)_3^-$  catalysts are capable of incorporating **MCH** and **MCP** into the polyethylene backbone, CGCTi $Me^+MeB(C_6F_5)_3^-$  catalysts enchain **MCH** and **MCP** into ethylene copolymers to form polymer structures **C** and **D**, respectively. An appealing

Scheme 6. Proposed Mechanistic Scenario for Enhanced MCA Enchainment by Bimetallic Catalyst FI<sup>2</sup>-Ti<sub>2</sub>

explanation is that tighter ion pairing in  $\text{CGCZrMe}^+\text{MeB}(\text{C}_6\text{F}_5)_3^-$  versus  $\text{CGCTiMe}^+\text{MeB}(\text{C}_6\text{F}_5)_3^-$  structures leads to lower bulky comonomer enchainment selectivity.<sup>14a,36</sup> A similar scenario may be operative in the present FI catalyst series. Thus, while FI<sup>2</sup>-Ti<sub>2</sub> and FI-Ti<sub>1</sub> incorporate MCH and MCP into ethylene copolymers with moderate activities as noted above, FI<sup>2</sup>-Zr<sub>2</sub> and FI-Zr<sub>1</sub> produce exclusively polyethylene homopolymer under the same reaction conditions. Tighter ion pairing between the Zr cation and the associated MAO anion could raise the barrier to coordination and insertion of the very bulky methylenecycloalkanes. For FI<sup>2</sup>-Ti<sub>2</sub>, it appears that one electrophilic Ti center assists the proximate Ti center in inserting the bulky MCA comonomers (Scheme 6). While MCP is incorporated in a very low percentage, MCH is incorporated to 11.6%, which is  $\sim 3.4\times$  the enchainment level achieved by FI-Ti<sub>1</sub>.

**V. Ethylene +  $\alpha,\omega$ -Diene Copolymerizations.** It is reasonable to assume that the copolymerizations of ethylene + 1,4-PD and ethylene + 1,5-HD follow essentially similar pathways to ethylene +  $\alpha$ -olefin copolymerizations with respect to the observed enhanced incorporation of comonomer (Schemes 1 and 3). In the case of FI<sup>2</sup>-Zr<sub>2</sub>- and FI-Zr<sub>1</sub>-catalyzed copolymerization of ethylene + 1,4-PD, 1,3-cyclohexyl units are

incorporated in polymer structure G (Chart 4) with 69% *cis*- and 82% *cis*-1,3-cyclohexyl group selectivity, respectively. In the case of FI<sup>2</sup>-Zr<sub>2</sub> and FI-Zr<sub>1</sub> catalyzed copolymerization of ethylene + 1,5-HD, 1,3-cyclopentyl units are enchainment to form polymer structure F (Chart 4) with 65% *cis*- and 44% *cis*-1,3-cyclohexyl group selectivity, respectively. No detectable cross-linked polymers are found in any of the product polymers. Interestingly, under identical reaction conditions, FI<sup>2</sup>-Ti<sub>2</sub> and FI-Ti<sub>1</sub> yield only trace amounts of copolymer. Regarding the differences in the *cis/trans* ratios in the polymer products obtained from FI<sup>2</sup>-Zr<sub>2</sub> and FI-Zr<sub>1</sub>, it is plausible that the proximate metal center in FI<sup>2</sup>-Zr<sub>2</sub> plays a role in directing the ring closure stereochemistry. Waymouth and Resconi<sup>37</sup> analyzed the transition states for 1,5-HD homopolymerization mediated by various zirconocenium catalysts differing in the bulkiness of the cyclopentadienyl ligands. They found, both in experiment and theory, that bulkier cyclopentadienyl ligands induce greater diastereoselectivity for *cis*-ring closure. They proposed that the selectivity for *trans*-ring formation reflects a preference for a chairlike transition state in which the polymer chain occupies an equatorial position (Figure 6a). However, as the ancillary ligand steric encumbrance increases, the chair-like transition-state is destabilized by the cyclopentadienyl ligand substituents,

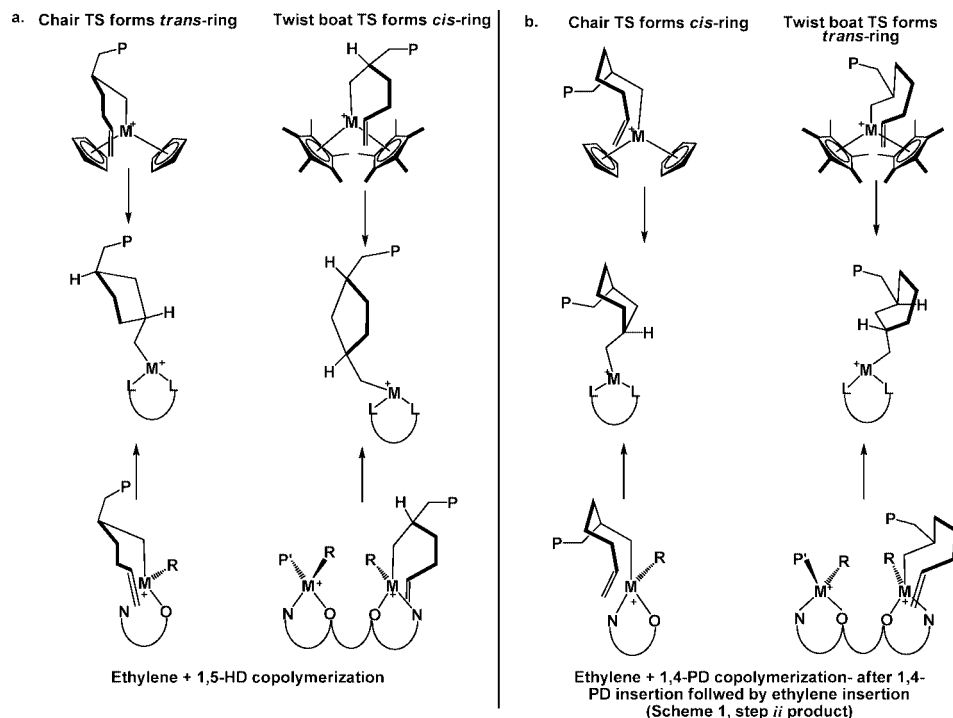


**Figure 6.** Transition states for cyclization of (a) 1,5-HD and (b) 1,4-PD catalyzed by metallocenium catalysts and by phenoxyiminato catalysts (ligand structures abbreviated for clarity; M = Ti, Zr; P = polymer chain; L = Cp, Me<sub>4</sub>Cp, FI, or FI<sup>2</sup>; R = alkyl, H).

**Table 3. Comparison of CGC Catalyst Properties<sup>5,13,22</sup> versus FI Catalyst Properties (Present Study) for Ethylene Homo- and Copolymerizations<sup>a</sup>**

	CGC catalysts	FI catalysts
activity	Ti: very high; Zr: moderate	Ti/Zr: moderate, with Zr being slightly greater
activity of mononuclear vs binuclear	Ti/Zr: bimetallics slightly less active than monometallics	Ti/Zr: bimetallics more active than monometallics
ethylene + $\alpha$ -olefin enchainment selectivity	~0.6% to 15% incorporation of $\alpha$ -olefins (0.6–0.8 M comonomer)	~4.0% to 15% enchainment of $\alpha$ -olefins (0.72 M comonomer)
ethylene + $\alpha$ -olefin enchainment mononuclear vs binuclear	<b>Ti<sub>2</sub></b> enchains ~3–7 $\times$ more $\alpha$ -olefin than <b>Ti<sub>1</sub></b> ; <b>Zr<sub>2</sub>/Cl-Zr<sub>2</sub></b> enchain ~3–12 $\times$ more $\alpha$ -olefin than <b>Zr<sub>1</sub></b>	<b>FI<sup>2</sup>-Ti<sub>2</sub>/FI<sup>2</sup>-Zr<sub>2</sub></b> enchain 1.5–2.2 $\times$ more $\alpha$ -olefin than <b>FI-Ti<sub>1</sub>/FI-Zr<sub>1</sub></b>
$M_w$ of ethylene + $\alpha$ -olefin product (10 <sup>3</sup> /mol)	Ti, 147–161; Zr, 0.24–380; Ti/Zr, $M_w$ increases with increasing nuclearity	Ti, 76–188; Zr, 21–105; <b>FI<sup>2</sup>-Zr<sub>2</sub></b> yields higher $M_w$ than <b>FI-Zr<sub>1</sub></b>
polyethylene $M_w$ (10 <sup>3</sup> /mol)	Ti, $M_w$ = 121–171; Zr, $M_w$ = 0.61–268; $M_w$ increases as catalyst nuclearity increases	Ti, 297–675; Zr, 155 and higher
polyethylene microstructure	<b>Ti<sub>2</sub>/Zr<sub>2</sub></b> : ethyl branching; <b>Ti<sub>1</sub></b> : linear with vinylic endgroups; <b>Zr<sub>1</sub></b> : long-chain branching with vinylic endgroups	Ti/Zr: linear with saturated and vinylic endgroups
ethylene + MCA enchainment selectivity	<b>Ti<sub>2</sub></b> enchains ~2 $\times$ more MCA than <b>Ti<sub>1</sub></b> ; Zr inactive for MCA copolymerization	<b>FI<sup>2</sup>-Ti<sub>2</sub></b> enchains 2–3 $\times$ more MCA than <b>FI-Ti<sub>1</sub></b> ; Zr inactive for MCA copolymerization
ethylene + MCA $M_w$ (10 <sup>3</sup> /mol)	$M_w$ = 158–320; <b>Ti<sub>2</sub></b> gives slightly lower $M_w$	$M_w$ = 20–121; <b>FI<sup>2</sup>-Ti<sub>2</sub></b> yields ~2–5 $\times$ higher $M_w$
predominant chain transfer mechanism	<b>Ti<sub>2</sub>/Zr<sub>2</sub>/Cl-Zr<sub>2</sub></b> : $\beta$ -hydride transfer to ethylene; <b>Ti<sub>1</sub>/Zr<sub>1</sub></b> - $\beta$ -hydride elimination with borane/borate cocatalysts	~50–70% chain transfer to Al and ~30–50% $\beta$ -hydride elimination
catalyst stability	very stable/long-lived	multiple active sites formed, then long-lived

<sup>a</sup> Unless otherwise noted, the polymerization conditions compared within each entry are identical. catalyst structures are given in Charts 1 and 3.

with an alternative twist-boat transition state placing the polymer chain in an equatorial position, leading to *cis*-1,3-cyclopentyl closure. Theoretical studies on the insertion pathways in CpTiCl<sub>3</sub>-derived catalysts, which may offer a closer comparison to the **FI-M<sub>1</sub>** and **FI<sup>2</sup>-M<sub>2</sub>** structures and coordination spheres, suggest similar pathways for insertion of dienes.<sup>38</sup> Comparing these proposed pathways with the present results leads us to suggest that the proximate metal in the bimetallic catalyst **FI<sup>2</sup>-Zr<sub>2</sub>** primarily serves as a bulky substituent which, in combination with possible agostic stabilization similar to that proposed for ethylene + olefin copolymerizations above (Schemes 4 and 5), leads to the greater *cis*-ring formation selectivity in the ethylene + **1,5-HD** copolymerizations versus **FI-Zr<sub>1</sub>** which is less sterically encumbered and hence less selective for *cis*-ring closure.

Applying the same diastereoselection mechanism to the ethylene + **1,4-PD** copolymerizations reported by Longo and co-workers,<sup>21</sup> **1,4-PD** insertion followed by ethylene insertion and cyclization should follow the same preferred pathway, i.e. a chairlike transition state with the polymer chain occupying an equatorial position. However, this transition state leads to *cis*-1,3-cyclohexyl ring closure (Figure 6b). If bulky ancillary ligands destabilize the chairlike transition state, a twist-boat transition state would then be preferred, forming a *trans*-1,3-cyclohexyl fragment. This opposite *cis/trans* selectivity relative to **1,5-HD** reflects the additional methylene unit involved in the ring closure. Hence, in Longo's study, the more encumbered *rac*-[CH<sub>2</sub>(3-*tert*-butyl-1-indenyl)<sub>2</sub>]ZrMe<sup>+</sup>MeMAO<sup>-</sup> zirconocenium catalyst displays greater selectivity for *trans*-1,3-cyclohexyl ring formation than does Cp<sub>2</sub>ZrMe<sup>+</sup>MeMAO<sup>-</sup> (Cp = cyclopentadienyl).<sup>21</sup> In the case of **FI<sup>2</sup>-Zr<sub>2</sub>** and **FI-Zr<sub>1</sub>**-catalyzed ethylene + **1,4-PD** copolymerization, 1,3-cyclohexyl units are enchainment to form polymer structure **G** (Chart 4) with 31% and 18% *trans*-1,3-cyclohexyl group selectivity, respectively. Following the trend that more encumbered catalysts lead to greater *trans*-1,3-cyclohexyl group selectivity, the proximate metal in **FI<sup>2</sup>-Zr<sub>2</sub>** may serve as a bulky group in the cycloinsertion process, in combination with stabilizing agostic interactions, leading to *trans*-1,3-cyclohexyl selectivity.

Interestingly, in both the mononuclear and the binuclear phenoxyiminato systems, the Zr catalysts exhibit much greater activity in ethylene +  $\alpha,\omega$ -diene copolymerizations than do the corresponding Ti catalysts, which have an activity <1 g polymer/[(mol M<sup>+</sup>) $\cdot$ atm $\cdot$ h]. In contrast, the ethylene + MCA copolymerizations follow the same trend as the CGC-**Zr<sub>2</sub>** and **-Ti<sub>2</sub>** catalysts in that **FI<sup>2</sup>-Zr<sub>2</sub>** and **FI-Zr<sub>1</sub>** do not enchain MCAs, while **FI<sup>2</sup>-Ti<sub>2</sub>** and **FI-Ti<sub>1</sub>** enchain MCAs to levels of 0.4% and 11.6%, respectively. If **FI<sup>2</sup>-Zr<sub>2</sub>** is involved in stronger ion pairing than **FI<sup>2</sup>-Ti<sub>2</sub>** (following the CGC-Zr and CGC-Ti

trend<sup>38</sup>), it is then plausible that the determining factor for diene copolymerization is that the catalyst be sufficiently coordinatively/sterically open. It is also plausible that the larger ionic radius of Zr(IV) versus Ti(IV) is required for diene coenchainment. Taken together, these two factors can explain why **FI<sup>2</sup>-Ti<sub>2</sub>** and **FI-Ti<sub>1</sub>** do not efficiently enchain dienes. In fact, to our knowledge, there are only two reports of a single-site Ti catalyst, [( $\eta^5$ -C<sub>5</sub>Me<sub>4</sub>)SiMe<sub>2</sub>(N<sup>t</sup>Bu)]TiCl<sub>2</sub>, incorporating a nonconjugated diene into an ethylene copolymer, and in neither case is the diene cyclized.<sup>39</sup>

**VI. Comparison of Mono- and Bimetallic CGC Catalysts to Phenoxyiminato Mono- and Bimetallic Catalysts.** The new family of bimetallic **FI<sup>2</sup>-M<sub>2</sub>** phenoxyiminato group 4 catalysts exhibit both similarities and differences versus the bimetallic CGC group 4 catalysts studied earlier. Table 3 summarizes these similarities and differences. Most notably, both families of bimetallic catalysts display dramatic selectivity effects in enhancing comonomer enchainment levels vs their monometallic analogues. In ethylene +  $\alpha$ -olefin copolymerizations mediated by **FI<sup>2</sup>-M<sub>2</sub>**, between 1.5-fold and 2.2-fold increases are achieved vs the copolymerizations mediated by **FI-M<sub>1</sub>**. These increases are relatively modest in comparison to the 12-fold increase in 1-octene incorporation achieved for **Ti<sub>2</sub>/B<sub>2</sub>** vs **Ti<sub>1</sub>/B<sub>1</sub>**.<sup>5c</sup> However, the percentage of 1-octene enchainment in the **Ti<sub>2</sub>/B<sub>2</sub>** case is 7.0%, while the percentage of 1-octene coenchainment for **FI<sup>2</sup>-Zr<sub>2</sub>** is 7.3% and that for **FI<sup>2</sup>-Ti<sub>2</sub>** is 15.2% under conditions only marginally more concentrated in 1-octene (0.72 M vs 0.64 M). This dramatic difference in comonomer incorporation is reasonably due to the nature of the **FI-M<sub>1</sub>** moiety which can facilitate the incorporation of sterically demanding olefin comonomers. This factor, in combination with the proposed agostic interactions involved between the alkyl chain of the olefin and the proximate metal, lead to high enchainment levels of 1-octene. In the ethylene + MCA copolymerizations mediated by both families of catalysts, only the Ti catalysts are competent to copolymerize MCAs with ethylene. As mentioned above, we tentatively attribute this to tighter ion pairing between the Zr cation and the associated MAO counteranion, which retards approach, coordination, and enchainment of bulky comonomers.<sup>14,38</sup> An important difference between the CGC and **FI** families of catalysts is the general trend observed for the bimetallic CGC catalysts to display *lower* polymerization activities than their mononuclear analogues, while the bimetallic **FI<sup>2</sup>-M<sub>2</sub>** catalysts display *higher* polymerization activities than their monometallic analogues. For example, ethylene + 1-hexene copolymerizations mediated by **Zr<sub>2</sub>/B<sub>1</sub>** display an activity 1.5 $\times$  lower than that of **Zr<sub>1</sub>/B<sub>1</sub>**,<sup>5g</sup> while, in contrast, **FI<sup>2</sup>-Zr<sub>2</sub>** displays 12 $\times$  greater activity than that of **FI-Zr<sub>1</sub>** for ethylene

+ 1-hexene copolymerizations. It was concluded that the decrease in activities observed for the bimetallic CGCs is due to the  $\alpha$ -olefin blocking/competing for active sites, especially for the higher nuclearity sites.<sup>5b</sup> A plausible argument for the observed increase in activity for the bimetallic  $\text{FI}^2\text{-M}_2$  catalysts is the coordinatively open nature of the active site. It may be that, in combination with the agostic interactions involving the proximate metal center, the  $\text{FI}^2\text{-M}_2$  coordination sphere is sufficiently open to avoid activity loss due to competition for enchainment sites.

Another major difference between the CGC and FI catalyst systems is the  $M_w$  of the (co)polymers produced by each family of catalysts. While CGC-Zr catalysts tend to form low  $M_w$  polymers, this characteristic can be substantially modified by proper choice of cocatalyst. Using MAO as the cocatalyst dramatically increases the product polymer  $M_w$  in  $\text{CI-Zr}_2$ -mediated ethylene homopolymerizations and ethylene + 1-hexene copolymerizations.<sup>3c,5b,d</sup> In the case of the FI catalyst family, molecular weights greater than 20 000 g/mol are obtained in all cases.

Branched polyethylene microstructures are also obtained in CGC-mediated ethylene homopolymerizations. Specifically, substantial ethyl branch densities are present in  $\text{Ti}_2\text{-Zr}_2$ ,  $\text{Zr}_2$ , and  $\text{CI-Zr}_2$ -derived ethylene homopolymers and are proposed to arise from  $\beta$ -hydride transfer from the growing polymer directly to metal-bound ethylene, followed by rapid reinsertion of olefin-terminated macromonomer. Also,  $\text{Zr}_1$  produces long-chain branched polyethylene by reinsertion of olefin-terminated macromonomers.<sup>5d</sup> In contrast, the FI-family of catalysts produces essentially branch-free, linear polyethylenes where ~68% of the polymer chains are terminated by chain transfer to Al (Scheme 3) and ~32% of the polymer chains are terminated by  $\beta$ -hydride elimination. Long-chain branches arising from macromonomer reinsertion are not detected in the <sup>1</sup>H and <sup>13</sup>C NMR spectra.

A last major difference in the two families of catalysts concerns the stabilities of their active sites. The CGCs are stable and long-lived even at higher temperatures,<sup>5</sup> whereas the FI-catalysts show broadened PDIs indicative of multiple active sites. These different active sites may arise from either of the ligand reaction or ligand rearrangement reactions mentioned above (eqs 5 and 6). A stable catalytic species should in theory have PDI = 2.0, however the PDIs of the (co)polymers in the current study range from 3.22 to 33.6.

## Summary

The binucleating phenoxyimine ligand  $\text{H}_2\text{-FI}^2$  and the corresponding bimetallic group 4 complexes  $\{1,8\text{-(O)}_2\text{C}_{10}\text{H}_4\text{-}2,7\text{-[CH=N(2,6-}^i\text{Pr}_2\text{C}_6\text{H}_3)_2]\text{Zr}_2\text{Cl}_6(\text{THF})_2$  ( $\text{FI}^2\text{-Zr}_2$ ) and  $\{1,8\text{-(O)}_2\text{C}_{10}\text{H}_4\text{-}2,7\text{-[CH=N(2,6-}^i\text{Pr}_2\text{C}_6\text{H}_3)_2]\text{Ti}_2\text{Cl}_6(\text{THF})_2$  ( $\text{FI}^2\text{-Ti}_2$ ) have been synthesized and characterized. The catalyst design focused on maximizing interactions between the two metal centers. We compared and contrasted the polymerization properties of these two catalysts with those of their mononuclear analogues,  $\text{FI-Ti}_1$  and  $\text{FI-Zr}_1$ , in ethylene homopolymerizations, ethylene +  $\alpha$ -olefin copolymerizations, ethylene + MCA copolymerizations, and ethylene +  $\alpha,\omega$ -diene copolymerizations. To our knowledge, this study represents first report of copolymerizations achievable with monophenoxyiminato group 4 catalysts and the second report of significant incorporation of MCAs into polyethylene backbones via a coordination polymerization process. Substantial increases in catalytic activity and comonomer enchainment efficiency into the polyethylene microstructure are observed for all comonomers versus the respective mononuclear catalyst analogues. It is also found that distinct comonomer selectivity differences are displayed for the Zr versus Ti catalysts. Thus, the Zr catalysts enchain  $\alpha,\omega$ -dienes

efficiently while the Ti catalysts are inactive for ethylene +  $\alpha,\omega$ -diene copolymerization. Conversely, the Ti catalysts enchain MCAs efficiently while the Zr catalysts are unable to enchain MCAs.

**Acknowledgment.** Financial support from NSF (Grant No. CHE-0809589) and DOE (Grant No. 86ER13511) is gratefully acknowledged. We thank Dr. A. Dash, Mr. M. Delferro, Dr. N. Guo, and Mr. B. Rodriguez for helpful discussions. We thank Mr. Z. Shen and Prof. R. F. Jordan for hospitality with GPC measurements.

**Supporting Information Available:** Text giving ligand, catalyst synthesis, and characterization procedures and polymerization experiments and polymer characterization, tables of crystal structure data and bond lengths and angles, and two cif files giving the details of the crystal structures. This material is available free of charge via the Internet at <http://pubs.acs.org>.

## References and Notes

- (1) For recent examples, see: (a) Esswein, A. J.; Veige, A. S.; Piccoli, P. M. B.; Schultz, A. J.; Nocera, D. G. *Organometallics* **2008**, *27*, 1073–1083. (b) Li, C.; Chen, L.; Garland, M. J. *Am. Chem. Soc.* **2007**, *129*, 13327–13334. (c) Weng, Z.; Teo, S.; Liu, Z.; Hor, T. S. A. *Organometallics* **2007**, *26*, 2950–2952. (d) Sammis, G. M.; Danjo, H.; Jacobsen, E. N. *J. Am. Chem. Soc.* **2004**, *126*, 9928–9929. (e) Moore, D. R.; Cheng, M.; Lobkovsky, E. B.; Coates, G. W. *J. Am. Chem. Soc.* **2003**, *125*, 11911–11924. (f) Trost, B. M.; Mino, T. *J. Am. Chem. Soc.* **2003**, *125*, 2410–2411. (g) Jacobsen, E. N. *Acc. Chem. Res.* **2000**, *33*, 421–431. (h) Molenveld, P.; Engbersen, J. F. J.; Reinhoudt, D. N. *Chem. Soc. Rev.* **2000**, *29*, 75–86. (i) Konsler, R. G.; Karl, J.; Jacobsen, E. N. *J. Am. Chem. Soc.* **1998**, *120*, 10780–10781. (j) Molenveld, P.; Kapsabelis, S.; Engbersen, J. F. J.; Reinhoudt, D. N. *J. Am. Chem. Soc.* **1997**, *119*, 2948–2949. (k) Mathews, R. C.; Howell, D. H.; Peng, W.-J.; Train, S. G.; Treleaven, W. D.; Stanley, G. G. *Angew. Chem., Int. Ed. Engl.* **1996**, *35*, 2253–2256. (l) Sawamura, M.; Sudoh, M.; Ito, Y. *J. Am. Chem. Soc.* **1996**, *118*, 3309–3310.
- (2) (a) Collman, J. P.; Boulatov, R.; Sunderland, C. J.; Fu, L. *Chem. Rev.* **2004**, *104*, 561–588. (b) Krishnan, R.; Voo, J. K.; Riordan, C. G.; Zahkarov, L.; Rheingold, A. L. *J. Am. Chem. Soc.* **2003**, *125*, 4422–4423. (c) Bruce, T. C. *Acc. Chem. Res.* **2002**, *35*, 139–148. (d) Bruce, T. C.; Benkovic, S. J. *Biochemistry* **2000**, *39*, 6267–6274, and references therein. (e) O'Brien, D. P.; Entress, R. M. N.; Matthew, A. C.; O'Brien, S. W.; Hopkinson, A.; Williams, D. H. *J. Am. Chem. Soc.* **1999**, *121*, 5259–5265. (f) Carazo-Salas, R. E.; Guarguaglini, G.; Gruss, O. J.; Segref, A.; Karsenti, E.; Mattaj, L. W. *Nature* **1999**, *400*, 178–181. (g) Menger, F. M. *Acc. Chem. Res.* **1993**, *26*, 206–212, and references therein. (h) Page, M. I. In *The Chemistry of Enzyme Action*; Page, M. I., Ed.; Elsevier: New York, 1984; pp 1–54.
- (3) For recent reviews of single-site olefin polymerization, see: (a) Marks, T. J. *Proc. Natl. Acad. Sci. U.S.A.* **2006**, *103* (Special Feature on Polymerization). (b) Li, H.; Marks, T. J. *Proc. Natl. Acad. Sci. U.S.A.* **2006**, *103*, 15295–15302. (c) Severn, J. R.; Chadwick, J. C.; Duchateau, R.; Friederichs, N. *Chem. Rev.* **2005**, *105*, 4073–4147. (d) Kaminsky, W. *J. Polym. Sci., Part A: Polym. Chem.* **2004**, *42*, 3911–3921. (e) Gibson, V. C.; Spitzmesser, S. K. *Chem. Rev.* **2003**, *103*, 283–316. (f) Pedoutour, J.-N.; Radhakrishnan, K.; Cramail, H.; Deffieux, A. *Macromol. Rapid Commun.* **2001**, *22*, 1095–1123. (g) Gladysz, J. A. *Chem. Rev.* **2000**, *100*, special issue on Frontiers in Metal-Catalyzed Polymerization). (h) Marks, T. J.; Stevens, J. C. *Top. Catal.* **1999**, *15*, and references therein. (i) Britovsek, G. J. P.; Gibson, V. C.; Wass, D. F. *Angew. Chem., Int. Ed.* **1999**, *38*, 428–447. (j) Kaminsky, W.; Arndt, M. *Adv. Polym. Sci.* **1997**, *127*, 144–187. (k) Bochmann, M. *J. Chem. Soc., Dalton Trans.* **1996**, 255–270. (l) Brintzinger, H.-H.; Fischer, D.; Mülhaupt, R.; Rieger, B.; Waymouth, R. M. *Angew. Chem., Int. Ed.* **1995**, *34*, 1143–1170. (m) *Catalyst Design for Tailor-Made Polyolefins*; Soga, K., Terano, M., Eds.; Elsevier: Tokyo, 1994. (n) Marks, T. J. *Acc. Chem. Res.* **1992**, *25*, 57–65.
- (4) For recent discussions of constrained-geometry catalysts, see: (a) Iedema, P. D.; Hoefsloot, H. C. J. *Macromolecules* **2003**, *36*, 6632–6644. (b) Klosin, J.; Kruper, W. J., Jr.; Nickias, P. N.; Roof, G. R.; De Waele, P.; Abboud, K. A. *Organometallics* **2001**, *20*, 2663–2665. (c) McKnight, A. L.; Waymouth, R. M. *Chem. Rev.* **1998**, *98*, 2587–2598. (d) Lai, S. Y.; Wilson, J. R.; Knight, G. W.; Stevens, J. C. *WO-93/08221*, **1993**.
- (5) (a) Guo, N.; Stern, C. L.; Marks, T. J. *J. Am. Chem. Soc.* **2008**, *130*, 2246–2261. (b) Li, H.; Li, L.; Schwartz, D. J.; Metz, M. V.; Marks,

- T. J.; Liable-Sands, L.; Rheingold, A. L. *J. Am. Chem. Soc.* **2005**, *127*, 14756–14768. (c) Li, H.; Stern, C. L.; Marks, T. J. *Macromolecules* **2005**, *38*, 9015–9027. (d) Li, H.; Li, L.; Marks, T. J. *Angew. Chem., Int. Ed.* **2004**, *43*, 4937–4940. (e) Li, H.; Li, L.; Marks, T. J.; Liable-Sands, L.; Rheingold, A. L. *J. Am. Chem. Soc.* **2003**, *125*, 10788–10789. (f) Li, L.; Metz, M. V.; Li, H.; Chen, M.-C.; Marks, T. J.; Liable-Sands, L.; Rheingold, A. L. *J. Am. Chem. Soc.* **2002**, *124*, 12725–12741.
- (6) *Spartan '06*; Wavefunction, Inc.: Irvine, CA, 2006. The dihedral angles about the alkyl bridge were constrained in order to identify the approximate, closest M...M distance.
- (7) For recent reviews, see: (a) Britovsek, G. J. P.; Gibson, V. C.; Wass, D. F. *Angew. Chem., Int. Ed.* **1999**, *38*, 428–447. (b) Ittel, S. D.; Johnson, L. K.; Brookhart, M. *Chem. Rev.* **2000**, *100*, 1169–1203. (c) Gibson, V. C.; Spitzmesser, S. K. *Chem. Rev.* **2003**, *103*, 283–316. (d) Suzuki, Y.; Terao, H.; Fujita, T. *Bull. Chem. Soc. Jpn.* **2003**, *76*, 1493–1517.
- (8) (a) Makio, H.; Kashiwa, N.; Fujita, T. *Adv. Synth. Catal.* **2002**, *344*, 477–493. (b) Suzuki, Y.; Terao, H.; Fujita, T. *Bull. Chem. Soc. Jpn.* **2003**, *76*, 1493–1517. (c) Tian, J.; Hustad, P. D.; Coates, G. W. *J. Am. Chem. Soc.* **2001**, *123*, 5134–5135.
- (9) (a) Pennington, D. A.; Clegg, W.; Coles, S. J.; Harrington, R. W.; Hursthouse, M. B.; Hughes, D. L.; Light, M. E.; Schormann, M.; Bochmann, M.; Lancaster, S. J. *Dalton Trans.* **2005**, *3*, 561–571. (b) Pennington, D. A.; Hughes, D. L.; Bochmann, M.; Lancaster, S. J. *Dalton Trans.* **2003**, *18*, 3480–3482. (c) Owin, D.; Parkin, S.; Ladipo, F. T. *J. Organomet. Chem.* **2003**, *678*, 134–141. (d) Goyal, M.; Mishra, S.; Singh, A. *Synth. React. Inorg. Met.-Org. Chem.* **2001**, *31*, 1705–1715.
- (10) (a) Arriola, D. J.; Carnahan, E. M.; Hustad, P. D.; Kuhlman, R. L.; Wenzel, T. T. *Science* **2006**, *312*, 714–719. (b) Mitani, M.; Saito, J.; Ishii, S.; Nakayama, Y.; Makio, H.; Matsukawa, N.; Matsui, S.; Mohri, J.; Furuyama, R.; Terao, H.; Bando, H.; Tanaka, H.; Fujita, T. *Chem. Rec.* **2004**, *4*, 137–158.
- (11) Salata, M. R.; Marks, T. J. *J. Am. Chem. Soc.* **2008**, *130*, 12–13.
- (12) *Spartan '06*; Wavefunction, Inc.: Irvine, CA, 2006. Assuming a planar metal–naphthyl–metal plane and M–N (Ti–N = 2.25 Å, Zr–N = 2.39 Å) and M–O (Ti–O = 1.82 Å, Zr–O = 1.95 Å) bond lengths equal to or greater than those identified crystallographically by Bochmann.<sup>9</sup>
- (13) Li, H.; Li, L.; Marks, T. J. *Angew. Chem., Int. Ed.* **2004**, *43*, 4937–4940.
- (14) (a) Jensen, T. R.; O'Donnell, J. J., III; Marks, T. J. *Organometallics* **2004**, *23*, 740–754. (b) Jia, L.; Yang, X. M.; Seyam, A. M.; Albert, I. D. L.; Fu, P. F.; Yang, S. T.; Marks, T. J. *J. Am. Chem. Soc.* **1996**, *118*, 7900–7913. (c) Jia, L.; Yang, X. M.; Marks, T. J. *J. Am. Chem. Soc.* **1996**, *118*, 1547–1548. (d) Yang, X. M.; Seyam, A. M.; Fu, P. F.; Marks, T. J. *Macromolecules* **1994**, *27*, 4625–4626. (e) Yang, X. M.; Jia, L.; Marks, T. J. *J. Am. Chem. Soc.* **1993**, *115*, 3392–3393.
- (15) (a) King, W. A.; Marks, T. J. *Inorg. Chim. Acta* **1995**, *229*, 343–354. (b) Schock, L. E.; Marks, T. J. *J. Am. Chem. Soc.* **1988**, *110*, 7701–7715.
- (16) (a) Takeuchi, D.; Anada, K.; Osakada, K. *Macromolecules* **2002**, *35*, 9628–9633. (b) Takeuchi, D.; Osakada, K. *Chem. Commun.* **2002**, *6*, 646–647. (c) Takeuchi, D.; Kim, S.; Osakada, K. *Angew. Chem., Int. Ed.* **2001**, *14*, 2685–2688.
- (17) (a) Kulshrestha, A. K.; Talapatra, S. In *Handbook of Polyolefins*; Vasile, C., Ed; Marcel Dekker: New York, 2000. (b) McKnight, A. L.; Waymouth, R. M. *Macromolecules* **1999**, *32*, 2816–2825. (c) Natori, I.; Imaizumi, K.; Yamagishi, H.; Kazunori, M. *J. Polym. Sci., Part B: Polym. Phys.* **1998**, *36*, 1657–1668. (d) Natori, I. *Macromolecules* **1997**, *30*, 3696–3697. (e) Cherdrón, H.; Brekner, M.-J.; Osan, F. *Angew. Makromol. Chem.* **1994**, *223*, 121–133. (f) James, D. E. In *Encyclopedia of Polymer Science and Engineering*; Marks, H. F., Bikales, N. M., Overberger, C. G., Menges, G., Eds.; Wiley-Interscience: New York, 1985; Vol. 6. (g) Zhao, J.; Hahn, S. F.; Hucul, D. A.; Meunier, D. M. *Macromolecules* **2001**, *34*, 1737–1741. (h) Hahn, S. F.; Hillmyer, M. A. *Macromolecules* **2003**, *36*, 71–76. (i) Ness, J. S.; Brodil, J. C.; Bates, F. S.; Hahn, S. F.; Hucul, D. A.; Hillmyer, M. A. *Macromolecules* **2002**, *35*, 602–609. (j) Gehlsen, M. D.; Weimann, P. A.; Bates, F. S.; Mays, J. J. *Polym. Sci., Part B: Polym. Phys.* **1995**, *33*, 1527–1536. (k) Gehlsen, M.; Bates, F. S. *Macromolecules* **1993**, *26*, 4122–4127.
- (18) Hucul, D. A.; Hahn, S. F. *Adv. Mater.* **2000**, *12*, 1855–1858.
- (19) Osakada, K.; Takeuchi, D. *Adv. Polym. Sci.* **2004**, *171*, 137–194.
- (20) (a) Resconi, L.; Waymouth, R. M. *J. Am. Chem. Soc.* **1990**, *112*, 4953–4954. (b) Coates, G. W.; Waymouth, R. M. *J. Am. Chem. Soc.* **1991**, *113*, 6270–6271. (c) Resconi, L.; Coates, G. W.; Mogstad, A.; Waymouth, R. M. *J. Macromol. Sci., Chem.* **1991**, *A28*, 1225–1234. (d) Naga, N.; Imanishi, Y. *Macromol. Chem. Phys.* **2002**, *203*, 771–777. (e) Pietikäinen, P.; Väinänen, T.; Seppälä, J. V. *Eur. Polym. J.* **1999**, *35*, 1047–1055. (f) Kokko, E.; Pietikäinen, P.; Koivunen, J.; Seppälä, J. V. *J. Polym. Sci.: Part A: Polym. Chem.* **2001**, *39*, 3805–3817. (g) Pietikäinen, P.; Seppälä, J. V.; Ahjopalo, L.; Pietilä, L.-O. *Eur. Polym. J.* **2000**, *36*, 183–192.
- (21) (a) Napoli, M.; Costabile, C.; Cavallo, G.; Longo, P. *J. Polym. Sci. Part A: Polym. Chem.* **2006**, *44*, 5525–5532. (b) Trifan, D. S.; Shelden, R. A.; Hoglen, J. J. *J. Polym. Sci. Part A: Polym. Chem.* **1968**, *6*, 1605–1614. (c) Napoli, M.; Costabile, C.; Pragliola, S.; Longo, P. *Macromolecules* **2005**, *38*, 5493–5497.
- (22) (a) Wang, J.; Li, H.; Guo, N.; Li, L.; Stern, C. L.; Marks, T. J. *Organometallics* **2004**, *23*, 5112–5114. (b) Abramo, G. P.; Li, L.; Marks, T. J. *J. Am. Chem. Soc.* **2002**, *124*, 13966–13967.
- (23) Glaser, T.; Liratzis, I. *Synlett.* **2004**, *4*, 735–737.
- (24) Wang, C.; Friedrich, S.; Younkin, T. R.; Li, R. T.; Grubbs, R. H.; Bansleben, D. A.; Day, M. W. *Organometallics* **1998**, *17*, 3149–3151.
- (25) (a) Fernandez-G, J. M.; del Rio-Portilla, F.; Zuiroz-Garcia, B.; Toscano, R. A.; Salcedo, R. *J. Mol. Struct.* **2001**, *561*, 197–207. (b) Ozeryanskii, V. A.; Pozharskii, A. F.; Schilf, W.; Kamieński, B.; Sawka-Dobrowolska, W.; Sobczyk, L.; Grech, E. *Eur. J. Org. Chem.* **2006**, *3*, 782–790.
- (26) Woodman, P. R.; Alcock, N. W.; Munslow, I. J.; Sanders, C. J.; Scott, P. *J. Chem. Soc., Dalton Trans.* **2000**, *19*, 3340–3346.
- (27) Liguori, D.; Centore, R.; Tuzi, A.; Grisi, F.; Sessa, I.; Zambelli, A. *Macromolecules* **2003**, *36*, 5451–5458.
- (28) See Supporting Information for details.
- (29) (a) Bott, R. K. J.; Hughes, D. L.; Schormann, M.; Bochmann, M.; Lancaster, S. J. *J. Organomet. Chem.* **2003**, *665*, 135–149. (b) Tohi, Y.; Makio, H.; Matsui, S.; Onda, M.; Fujita, T. *Macromolecules* **2003**, *36*, 523–525. (c) Woodman, P. R.; Alcock, N. W.; Munslow, I. J.; Sanders, C. J.; Scott, P. *J. Chem. Soc., Dalton Trans.* **2000**, *19*, 3340–3346.
- (30) (a) Nabhrain, N.; Brintzinger, H.-H.; Ruchatz, D.; Fink, G. *Macromolecules* **2005**, *38*, 2056–2063. (b) Makio, H.; Koo, K.; Marks, T. J. *Macromolecules* **2001**, *34*, 4676–4679. (c) Byun, D. J.; Shin, D. K.; Kim, S. Y. *Polym. Bull. (Berlin)* **1999**, *42*, 301. (d) Leino, R.; Luttikhedde, H. J. G.; Lehmus, P.; Willen, C.; Sjöholm, R.; Lehtonen, A.; Seppälä, J.; Nasman, J. H. *Macromolecules* **1997**, *30*, 3477–3483. (e) Rieger, B.; Reinmuth, A.; Roll, W.; Brintzinger, H. H. *J. Mol. Catal.* **1993**, *82*, 67. (f) Resconi, L.; Piemontesi, F.; Franciscono, G.; Abis, L.; Fiorani, T. *J. Am. Chem. Soc.* **1992**, *114*, 1025–1032. (g) Mogstad, A. L.; Waymouth, R. M. *Macromolecules* **1992**, *25*, 2282–2284.
- (31) Saito, J.; Tohi, Y.; Matsukawa, N.; Mitani, M.; Fujita, T. *Macromolecules* **2005**, *38*, 4955–4957.
- (32) Pooter, M. D.; Smith, P. B.; Dohrer, K. K.; Bennett, K. F.; Meadows, M. D.; Smith, C. G.; Schouwenaars, H. P.; Geerards, R. A. *J. Appl. Polym. Sci.* **1991**, *42*, 399–408.
- (33) Naga, N.; Imanishi, Y. *Macromol. Chem. Phys.* **2002**, *203*, 771–777.
- (34) (a) Scherer, W.; McGrady, G. S. *Angew. Chem., Int. Ed.* **2004**, *43*, 1782–1806. (b) Proscenc, M. H.; Brintzinger, H. H. *Organometallics* **1997**, *16*, 3889–3894. (c) Grubbs, R. H.; Coates, G. W. *Acc. Chem. Res.* **1996**, *29*, 85–93. (d) Proscenc, M. H.; Janiak, C.; Brintzinger, H. H. *Organometallics* **1992**, *11*, 4036–4041. (e) Cotter, W. D.; Bercaw, J. E. *J. Organomet. Chem.* **1991**, *417*, C1–C6. (f) Krauledat, H.; Brintzinger, H. H. *Angew. Chem., Int. Ed. Engl.* **1990**, *29*, 1412–1413. (g) Piers, W. E.; Bercaw, J. E. *J. Am. Chem. Soc.* **1990**, *112*, 9406–9407. (h) Brookhart, M.; Green, M. L. H.; Wong, L. L. *Prog. Inorg. Chem.* **1988**, *36*, 1–124. (i) Clawson, L.; Soto, J.; Buchwald, S. L.; Steigerwald, M. L.; Grubbs, R. H. *J. Am. Chem. Soc.* **1985**, *107*, 3377–3378.
- (35) (a) Motta, A.; Fragala, I. L.; Marks, T. J. Theoretical Investigation of Proximity Effects in Binuclear Catalysts for Olefin Polymerization. Poster Presentation at the International Symposium on Relationships between Heterogeneous and Homogeneous Catalysis XIII, Berkeley, CA, July 16–20, 2007. (b) Motta, A.; Fragala, I. L.; Marks, T. J. *J. Am. Chem. Soc.*, in press.
- (36) (a) Glaser, T.; Liratzis, I.; Fröhlich, R.; Weyhermüller, T. *Chem. Commun.* **2007**, *4*, 356–358. (b) Glaser, T.; Liratzis, I.; Fröhlich, R. *Dalton Trans.* **2005**, *17*, 2892–2898.
- (37) Horton, A. D. *Organometallics* **1996**, *15*, 2675–2677.
- (38) Luo, L.; Marks, T. J. *Top. Catal.* **1999**, *7*, 97–106.
- (39) (a) Coates, G. W.; Waymouth, R. M. *J. Am. Chem. Soc.* **1993**, *115*, 91–98. (b) Cavallo, L.; Guerra, G.; Corradini, P.; Resconi, L.; Waymouth, R. *Macromolecules* **1993**, *26*, 260–267.
- (40) (a) Peluso, A.; Improta, R.; Zambelli, A. *Organometallics* **2000**, *19*, 411–419. (b) Peluso, A.; Improta, R.; Zambelli, A. *Macromolecules* **1997**, *30*, 2219–2227.
- (41) (a) Santos, J. M.; Ribeiro, M. R.; Portela, M. F.; Cramail, H.; Deffieux, A.; Antão, A.; Otero, A.; Prashar, S. *Macromol. Chem. Phys.* **2002**, *203*, 139–145. (b) Santos, J. M.; Ribeiro, M. R.; Portela, M. F.; Cramail, H.; Deffieux, A. *Macromol. Chem. Phys.* **2001**, *202*, 3043–3048.